DISSERTATIONES
CHIMICAE
UNIVERSITATIS
TARTUENSIS
208

OLIVIER ETEBE NONGA

Inhibitors and photoluminescent probes for *in vitro* studies on protein kinases PKA and PIM

DISSERTATIONES CHIMICAE UNIVERSITATIS TARTUENSIS
208

DISSERTATIONES CHIMICAE UNIVERSITATIS TARTUENSIS
208

OLIVIER ETEBE NONGA

Inhibitors and photoluminescent probes for *in vitro* studies on protein kinases PKA and PIM

UNIVERSITY OF TARTU
Press
1632

Institute of Chemistry, Faculty of Science and Technology, University of Tartu, Estonia

Dissertation was accepted for defense of the degree of Doctor of Philosophy in Chemistry by the Council of Institute of Chemistry, Faculty of Science and Technology, University of Tartu on August 27th, 2021.

Supervisors: Asko Uri, PhD
Professor, Institute of Chemistry, University of Tartu

Erki Enkvist, PhD
Associate Professor, Institute of Chemistry,
University of Tartu

Opponent: Harri Härmä, PhD
University Lecturer, Laboratory of Materials Chemistry and Chemical Analysis (Department of Chemistry), University of Turku, Finland

Commencement: October 26th, 2021 at 14:15, room 1020, 14A Ravila St., Institute of Chemistry, University of Tartu

This research was supported by grants from the Estonian Research Council (PRG454 and IUT20-17), from EU ERA-NET TRANSCAN-2 (project PROSCANEXO), and Graduate School of Functional materials and technologies receiving funding from the European Regional Development Fund in University of Tartu, Estonia.

ISSN 1406-0299
ISBN 978-9949-03-700-1 (print)
ISBN 978-9949-03-701-8 (pdf)

University of Tartu Press
www.tyk.ee

CONTENTS

LIST OF ORIGINAL PUBLICATIONS 7

ABBREVIATIONS 8

1. INTRODUCTION 10

2. LITERATURE OVERVIEW 11
   - 2.1. Protein kinases 11
     - 2.1.1. cAMP-dependent protein kinase 11
     - 2.1.2. PIM kinases 12
   - 2.2. Antibodies 13
   - 2.3. Photoluminescence 15
     - 2.3.1. Förster-type resonant energy transfer 16
   - 2.4. Inhibitors of PKs 17
     - 2.4.1. Monofunctional inhibitors 18
     - 2.4.2. Bifunctional inhibitors 19
   - 2.5. Methods for studying inhibitor/PK complexes 21
     - 2.5.1. Activity and characterization of inhibitors 21
     - 2.5.2. Thermodynamics of inhibitor/PK binding 23
     - 2.5.3. Immunosorbent assays 24
     - 2.5.4. X-ray crystallographic studies and ligand binding modes 24

3. AIMS OF THE STUDY 27

4. METHODS 28
   - 4.1. Competitiveness of mAb(D38C6) and ARC for binding to PKAcα1 28
   - 4.2. Biochemical assays with measurement of FA or TGLI 28
   - 4.3. Co-crystallization, diffraction data collection, and structure determination 29
   - 4.4. Solid phase peptide synthesis 29
   - 4.5. Surface sandwich assay for PIM-2 measurement 30

5. SUMMARY OF RESULTS AND DISCUSSIONS 31
   - 5.1. Conformational rearrangements in PKAc (Paper I and unpublished data) 31
     - 5.1.1. Discovery of inhibitory properties of the antibody mAb(D38C6) against PKAcα1 31
     - 5.1.2. TGL properties of ARC-1085 and ARC-1086 in complex with PKAcβ1 and S54L-PKAcβ1 33
   - 5.2. Development of wild-type-sparing inhibitors for S54L-PKAcβ (Paper II and unpublished data) 35
   - 5.3. Inhibitors and probes for PIM kinases (Paper III) 39
     - 5.3.1. Co-crystal structures ARC-1411 and ARC-3126 with PIM-1 .. 39
     - 5.3.2. Design of new inhibitors and their characterization 41
   - 5.4. Development of assays for PKAcα and PIM-2 (Papers I, III, and unpublished data) 43

5.4.1. The AbARC assay 43
5.4.2. Surface sandwich assay for the measurement of PIM-2 concentration (AbARC-2 assay) 46
6. CONCLUSIONS 49
REFERENCES 50
SUMMARY IN ESTONIAN 60
ACKNOWLEDGEMENTS 62
PUBLICATIONS 63
CURRICULUM VITAE 177
ELULOOKIRJELDUS 178

LIST OF ORIGINAL PUBLICATIONS

The current thesis is based on the following original publications, referred to in the text by corresponding Roman numerals:

I. **O. E. Nonga**, D. Lavogina, T. Ivan, K. Viht, E. Enkvist, and A. Uri, "Discovery of strong inhibitory properties of a monoclonal antibody of PKA and use of the antibody and a competitive photoluminescent orthosteric probe for analysis of the protein kinase," *Biochimica et Biophysica Acta (BBA) – Proteins and Proteomics*, vol. 1868, no. 8, p. 140427, Aug. 2020.

II. **O. E. Nonga**, E. Enkvist, F. W. Herberg, and A. Uri, "Inhibitors and fluorescent probes for protein kinase PKAcβ and its S54L mutant, identified in a patient with cortisol producing adenoma," *Bioscience, Biotechnology, and Biochemistry*, vol. 84, no. 9, pp. 1839–1845, Sep. 2020.

III. **O. E. Nonga**, D. Lavogina, E. Enkvist, K. Kestav, A. Chaikuad, S. E. Dixon-Clarke, A. N. Bullock, S. Kopanchuk, T. Ivan, R. Ekambaram, K. Viht, S. Knapp, and A. Uri, "Crystal structure-guided design of bisubstrate inhibitors and photoluminescent probes for protein kinases of the PIM family," *Molecules*, vol. 26 , no. 14, pp. 4353, Jul. 2021.

Author's contribution:

Paper I: The author participated in planning the experiments, optimized and applied the developed assay, and participated in writing the manuscript. Compounds used in the study were synthesized by co-authors.

Paper II: The author participated in planning the experiments, performed all the biochemical experiments, interpreted the results, and participated in writing the manuscript. Compounds used in the study were synthesized by co-authors.

Paper III: The author participated in planning the experiments, performed most of the biochemical characterization of the compounds, and wrote the original draft of the manuscript. New compounds used in the study were synthesized by author.

ABBREVIATIONS

5-TAMRA	5-carboxytetramethylrhodamine
AA	amino acid
AbARC	photoluminescence immunoaffinity assay for PKAcα analysis
AbARC-2	photoluminescence ARC-affinity assay for PIM-2 analysis
Adc	adenosine 4’-dehydroxymethyl-4’-carboxylic acid moiety
AF647	Alexa Fluor 647® dye
Ahp	7-aminoheptanoic acid moiety
Ahx	6-aminohexanoic acid moiety
Aoc	8-aminooctanoic acid moiety
AMTH	5-(2-aminopyrimidin-4-yl)-thiophene-2-carboxylic acid moiety
ARC	adenosine analog and peptide mimetics conjugate
ARC-Lum	ARC-type probe possessing protein-induced luminescence when in complex with protein kinase
ARC-Lum(Fluo)	ARC-Lum probe conjugated with a fluorescent dye
ATP	adenosine-5’-triphosphate
AMP-PNP	β,γ-imidoadenosine-5′-triphosphate
BBTP	8-bromo-2-(methylene)[1]benzothieno[3,2-d]pyrimidin-4-one moiety
BPTP	7-bromo-2-(methylene)pyrido[4,5]thieno[3,2-d]pyrimidin-4-one moiety
cAMP	cyclic adenosine 3’,5’-monophosphate
CS	Cushing’s syndrome
Cyanine 5	2-[5-(1,3,3-Trimethylindoline-2-ylidene)-1,3-pentadienyl]-3,3-dimethyl-3H-indolium-1-hexanoic acid
D1D2	rabbit monoclonal antibody against PIM-2 (clone D1D2)
DIPEA	N,N-Diisopropylethylamine
DMF	N,N-dimethylformamide
FA	fluorescence anisotropy
FDA	U.S. Food and Drug Administration
FRET	Förster-type resonant energy transfer
HBTU	O-(benzotriazol-1-yl)-N,N,N’,N’-tetramethyluronium hexafluorophosphate
HEPES	4-(2-hydroxyethyl)-1-piperazineethanesulfonic acid
HOBt	1-hydroxybenzotriazole
HPLC	high performance liquid chromatography
IC_{50}	half maximal inhibitory concentration
IWC	index of wild-type–sparing capability
K_D	equilibrium dissociation constant determined by direct binding
mAb(D38C6)	rabbit monoclonal antibody against PKAcα (clone D38C6)

MW	molecular weight
NMM	N-methylmorpholine
PDB	Protein Data Bank
PIM	proviral integration site for Moloney murine leukemia virus
PK	protein kinase
PKA	cAMP-dependent protein kinase A holoenzyme
PKAc	catalytic subunit of PKA
PKAr	regulatory subunit of PKA
QY	quantum yield
TFA	trifluoroacetic acid
TGLI	time-gated luminescence intensity
TIPS	triisopropylsilane
WC	wild-type–sparing capability

1. INTRODUCTION

Phosphorylation reaction is an important cellular post-translational protein modification procedure that is catalyzed by protein kinases (PKs). Phosphorylation diversifies the proteome realm in influencing various aspects of normal and pathological physiology. Aberrant activity of PKs may be an indication or a cause of multiple complex diseases, such as cancer, diabetes, and cardiovascular diseases [1]. Therefore, PKs have become important drug targets in the 21st century. In last 22 years, more than 71 small-molecule drugs with reported inhibitory potency toward one or several PKs have been approved by the U.S. Food and Drug Administration (FDA) for clinical use. Besides, three PKs have been reported to be targetable to block SARS-CoV-2 entry in host cells [2] in an attempt to tackle COVID-19.

The number of human PKs catalyzing phosphorylation is 518. They constitute almost 2.5% of proteins coded by the human genome [3]. In addition to being potential drug targets, some PKs serve as biomarkers for cancers and other diseases since altered expression level or activity of various PKs are observed in a variety of malignancies [4]. Thus, there is a growing demand of analytical methods to determine the expression level and activity of disease-driving PKs. Besides, high throughput assays for screening PK inhibitors also form an important component of drug development pipeline.

ARC inhibitors (conjugates of adenosine analogs and peptide mimetics) are middle-sized flexible compounds. Discovery of the competitive nature of binding of ARCs and the commercial PKAcα antibody mAb(D38C6) to PKAcα enabled the development of a specific and sensitive assay for determination of kinase concentration in cell lysates. In this thesis, fluorescence anisotropy (FA)- and time-gated luminescence intensity (TGLI)-based assays were developed for analyzing PKAcβ, a PK involved in formation of the Cushing's syndrome (CS). Furthermore, moderately wild-type – sparing inhibitors for S54L-PKAcβ were constructed. Considering the impact that structural information may provide to the drug discovery iterative process [5], the first co-crystal structure of PIM kinase with ARC inhibitors were resolved and described herein. From these data, new inhibitors with optimized structures were constructed and their derivative compounds were applied in diverse assays.

2. LITERATURE OVERVIEW

2.1. Protein kinases

Protein phosphorylation was discovered by Krebs and Fischer in 1955 [6]. Phosphorylation has been found to be a common post-translational modification with 500,000 potential phosphorylation sites in the human proteome and 25,000 phosphorylation events described for 7,000 human proteins [7]. Protein phosphorylation is catalyzed by PKs, which catalyze the addition of γ-phosphate group from a nucleoside triphosphate (usually ATP) to the protein substrate. The addition of negative charges to the substrate protein changes its conformation, activity, and localization. Thus, it affects the processes that are downstream in the signaling cascade. PKs form one of the largest and most important "super-families" of proteins, encoded by 2.5% of all human genes [3]. The 518 human PKs have been classified into 8 groups according to sequence similarity of catalytic domains, the presence of accessory domains, and by considering modes of regulation. These groups are AGC, CAMK, CK1, CMGC, RGC, STE, TK, and TKL. Most PKs share a common eukaryotic PK catalytic domain. The remaining atypical PKs belong to several families, some of which have structural, but not sequence similarity to eukaryotic PKs [8]. Additionally, PKs have been also categorized as Ser/Thr or Tyr specific (phosphorylating) kinases. In fact, these phosphorylatable residues are asymmetrically distributed in proteome (85% Ser, 11.8% Thr, and 1.8% Tyr residues) [9]. The phosphorylation of Ser or Thr residues is mostly related to metabolism control (*e.g.* of Ser/Thr PKs , AGC kinases, CAMK kinases, *etc.*); phosphorylation of Tyr residues is mainly related to cell growth and division (*e.g.* of Tyr PKs: ABL kinases, SRC kinases, *etc.*). Dual specific kinases can act as both Ser/Thr and Tyr kinases (*e.g.*, DYRK, MAPK). There are some other kinases that phosphorylate side chains of other residues in proteins [10].

2.1.1. cAMP-dependent protein kinase

cAMP-dependent protein kinase (PKA) mediates many physiological responses in cells. For instance, it is a key player in steroidogenesis. PKA belongs to the AGC group [11] of PKs (63 members), comprising closely related PKs PKA, PKG, and PKC. PKA is a tetrameric enzyme composed of a dimer of regulatory (PKAr) subunits and dimer of catalytic (PKAc) subunits [12]. Binding of 2 cAMP molecules to each PKAr molecule activates the dissociation of the tetrameric inactive holoenzyme and subsequent phosphorylation of substrates by enzymatically active PKAc subunits [13]. The second messenger cAMP is always following activation of adenylate cyclase downstream of G protein-coupled receptors. In humans, PKAr possesses 4 isoforms (PKArIα, PKArIβ, PKArIIα, and PKArIIβ) and PKAc has four isozymes (PKAcα, PKAcβ, and PKAcγ, and PrKX). PKAr binds the A kinase anchoring proteins (AKAPs),

which anchor the holoenzyme at a specific cellular location [13], [14]. Besides, mutations in PKAc and PKAr have been associated with several pathologies [15], [16]. The point mutation L205R in the gene *PRKACA* encoding PKAcα was found in up to 67% of patients suffering from CS [15]. The point mutation S54L in the gene *PRKACB* encoding PKAcβ was recently found in a female patient with severe CS [16]. PKAc being a Ser/Thr PK, its selectivity to Ser phosphorylation is altered by the Phe187V mutation [17]. Substrates with a phosphorylatable Ser residue form a stable Michaelis complex with wild-type PKAc. Furthermore, PKA is an established biomarker in cancer [18], [19].

Human PKAcα has 2 splice variants producing the isoforms PKAcα1 and PKAcα2. PKAcα1 is ubiquitously expressed and PKAcα2 is sperm specific [20]. PKAcα1 has been extensively studied, it was the first PK to be crystallized, and has served a model for studying other PKs [21]. Roughly 70% of the sequence of the PKAc is shared by all PKs [21]. Human PKAcβ has 10 isoforms from 10 splice variants, which are PKAcβ1, PKAcβ2, PKAcβ3, PKAcβ4, PKAcβ3a, PKAcβ3ab, PKAcβ3abc, PKAcβ4a, PKAcβ4ab, and PKAcβ4abc [22], [23]. PKAcβ1 is most abundant in the brain, with low expression level in kidney. PKAcβ2 is the largest subunit among all PKAc possessing MW of 46 kDa, whereas both PKAcα1 and PKAcβ1 have MW of 41 kDa. PKAcβ4ab and PKAcβ4abc are human isoforms not identified in any other species [22] so far. In addition to the release from the PKAr, the catalytic activity of PKAc is realized only after two phosphorylation events within its structure: autophosphorylation at Ser338 and phosphorylation of Thr197 by PDK1. Free and catalytically active PKAc catalyze the phosphorylation of roughly 100 protein targets [24], including CREB at Ser133 with an ATP K_M value of 11.2 μM [25]. Although PKAcα and PKAcβ not being functionally redundant [23], viruses can use them similarly for their invasion into HEK293 cells and mice [26].

2.1.2. PIM kinases

The PIM family of PKs includes three constitutively active Ser/Thr kinases PIM-1, PIM-2, and PIM-3 that all regulate key biological processes from differentiation to apoptosis [27]. They belong to the calcium/calmodulin-dependent group (CAMK) of PKs (74 members) and are mostly localized in the cytosol and nucleus. PIM kinases are tightly regulated at both transcriptional and translational levels. There is a diversity of signals leading to PIM gene expression, *e.g.* cytokines, growth factors, and mitogenic stimuli in different cell types [28]. Janus kinase/signal transducer and activator of transcription and nuclear factor κB pathway activation are among the most extensively studied PIM upstream regulators. Nevertheless, PIM-1 phosphorylation at residue Tyr218 by Tyrosine-protein kinase Etk correlates with an increase in PIM-1 activity [29]. PIM kinases phosphorylate roughly 33 protein targets [30], including pro-apoptotic protein BAD at multiple sites [31]. PIM genes encodes different isozymes. PIM-1 is expressed primarily in cells of the hematopoietic and germline

lineages and is represented by 33- and 44-kDa isoforms [32]. PIM-2 is widely expressed and is represented by 34-, 38-, and 40-kDa isoforms. PIM-3 is detected in various tissues and is represented by its 36-kDa isoform. The different isoforms of PIM-1 and PIM-2 are encoded by genes having alternate translation initiation codons.

Within its catalytic domain, human Pim-2 is only 61% and 66% identical to PIM-1 and PIM-3, respectively. Besides, substrate specificity is also determined by the presence of disfavoring residues in the substrate recognition sequence of PKs. An example of this specificity is the presence of Pro at the P + 1 position, ensuring orthogonal substrate specificity between proline-directed PKs and PKs of the AGC or CAMK groups [33]. Consensus recognition sequences of PIM kinases and PKAc subunits are Arg-X-Arg-His-Pro-Ser/Thr-Gly [34], [35] and Arg-Arg/Lys-X-Ser/Thr-Leu/Ile [36], respectively, where X denotes any residue except Asp and Glu. In effect, based on these consensus sequences or the specificity determinants, PIM kinases and PKAc are members of basophilic PKs (preferring basic and hydrophobic amino acids as the determinants). Michaelis-Menten constant (K_M) values for ATP and Kemptide or Pimtide are reported in Table 1. PIM-related kinases in roundworm have been found to regulate sensory functions [37]. Due the elevated expression of PIM kinases in hematologic cancers, they can serve as disease biomarkers [38]. Furthermore, knockout of all PIM kinases leads to impairment in multiple lineages of hematopoietic cells [39]. Finally, PIM-1 and PIM-3 have redundant functions for promoting viral invasion, whereas PIM-2 does not promote this process due to poor binding to the target protein substrate [40].

Table 1. K_M^{app} values for ATP for PKAcα and PIM kinases and K_M^{app} values for Kemptide or Pimtide for PKAcα or PIM kinases, respectively

PK	K_M^{app} (ATP), μM	K_M^{app} (Kemptide or Pimtide), μM
PKAcα	17± 5[a]	20 ± 8 [a]
PIM-1	400 [b]	0.034 [c]
PIM-2	4 [b]	1.2 [c]
PIM-3	40 [b]	n. d.

K_M^{app} – apparent Michaelis-Menten constant; n. d. – not determined; a – ref. [41]; b – ref. [42]; c – ref. [34].

2.2. Antibodies

Antibodies belong to the group of Y-shaped antigen-binding proteins called immunoglobulins (Ig) that are produced by B-lymphocytes (B-cells) as an immunological response to an antigen. Antibodies can recognize specifically an amino acid sequence in an antigen molecule termed epitope. Antibodies consist

of two identical light (L) chains and heavy (H) chains that are linked together by disulfide bridges. The H chains α, δ, ε, γ, and μ determine the class or isotype where the antibody belongs: IgA, IgD. IgE, IgG, and IgM, respectively. Among Ig-s, IgG is the most abundant antibody in humans. IgG can be split into 4 sub-isotypes, each with its own effector function [43]. The 150-kDa IgG molecule consists of two identical 50-kDa H chains and two identical 25-kDa L chains (Figure 1; [44]). Antibodies can also be divided into monoclonal and polyclonal, where polyclonal antibodies are a mixture of antibodies that are produced by different B-cells. Monoclonal antibodies are produced by single B-cells; therefore, they all bind the same epitope [43]. The first 100–110 amino acids (variable region, Fv) of the amino terminal region of the L or H chain differ among antibodies of different specificity. The amino acid sequence beyond the variable region is constant in all antibody isotypes and it is termed the constant (crystallizable, Fc) region.

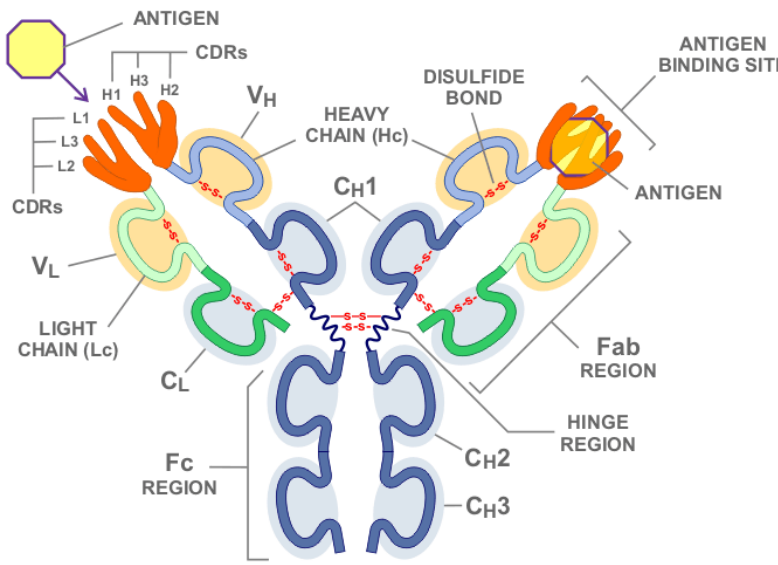

Figure 1. Structure of an immunoglobulin G

Primary Ig-s are raised against an epitope in a host species while secondary Ig-s are produced in another host against the Fc region's isotypes of the first species. The antigen binding site of an antibody (paratope) is located at the top of each of the two outstretched arms (Figure 1). Each site is defined by 6 loops called complementarity determining regions (CDR). There are 3 CDRs found on H chain (H1, H2, and H3) and 3 on the L chain (L1, L2, and L3) [43], [44]. These protein loops complement the shape and amino acid sequence of specific

antigens. As a result, they determine the specific antigens to which the antibody can and will bind. Besides, vaccination studies have provided proof-of-concept that antibodies can protect against viral challenge. However, the efficacy of most promising HIV vaccine trials to date is modest. Antibody-drug conjugates are a class of biopharmaceutical drugs designed as a targeted therapy that have proven efficient for treating cancers. Besides, therapeutic DNA-encoded monoclonal antibodies can be produced *in vivo* and they reduce the facing challenges of repeatedly administrating antibodies such as pre-existing immunity, difficult manufacturing processes, or high cost [45].

2.3. Photoluminescence

Research technologies based on the application of photoluminescence (e.g., spectrometry, microscopy, cell sorting) are gaining ever-growing importance in biomedical studies [46]. Photoluminescence is an optical emission of photons from a molecule that was photoexcited to a higher energy level. As a photoluminescent molecule (luminophore) absorbs a photon, its outer electrons are raised from the ground state (S_0) to some of its higher energy levels (S_1 or S_2) (Figure 2). After spending some time in the electronically excited state, the luminophore returns to the ground state either by emitting a photon (fluorescence) or by any of the following nonradiative processes: nonradiative dissipation of energy (as heat), intersystem crossing (ISC) to triplet state, resonance energy transfer (RET) to another molecule, photobleaching (light-induced destruction of a dye while in the excited state), *etc.* (Figure 2). Upon ISC, the electron in excited triplet state (T_1) changes its spin orientation to be the same as that of the electron that stays in the ground state (S_0). The emission from T_1 to S_0 (a forbidden process) is termed phosphorescence [47]. The average fluorescence lifetime or decay time (τ), i.e., the average time that the luminophore spends in the excited state before emitting a photon, is typically in the order of nanoseconds (1–10 ns) for organic fluorophores, whereas the phosphorescence lifetime is typically in the range from milliseconds to seconds. The relatively slow radiative decay from T_1 to S_0 if compared to nonradiative deactivation of T_1 causes the very low phosphorescence quantum yield (QY), i.e., the number of the emitted photons relative to the number of absorbed photons. Heavy atoms in the structure of the luminophore have positive effect on the transfer to T_1 and phosphorescence emission [48]. Phosphorescence and fluorescence QY-s can be increased by decreasing the temperature leading to slower nonradiative decay [47]. “Self-healing” fluorophores have low constant rates of nonradiative processes, thus high QY.

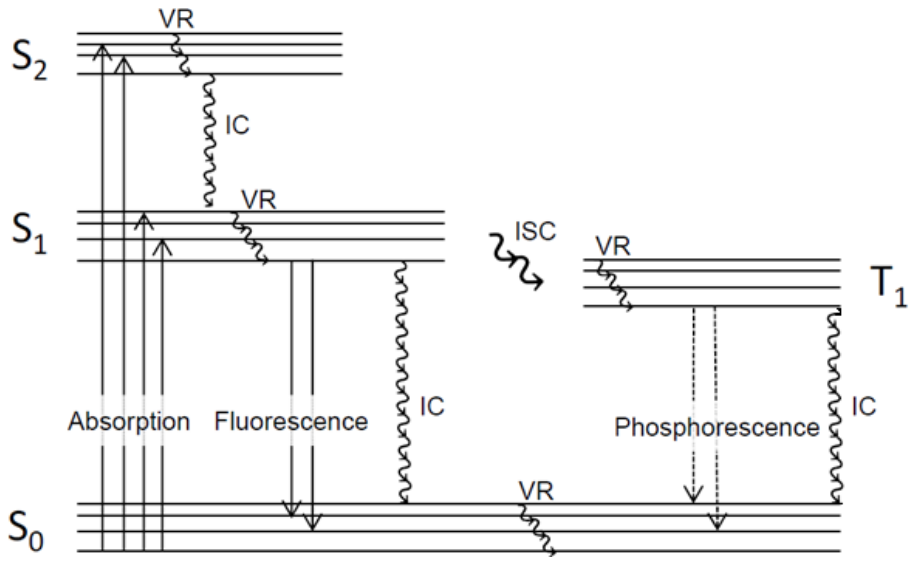

Figure 2. A version of the Jablonski diagram. S_0, ground singlet state; S_1, first excited singlet state; S_2, second excited singlet state; T_1, first excited triplet state; IC, internal conversion; ISC, intersystem crossing; VR, vibrational relaxation.

2.3.1. Förster-type resonant energy transfer

Förster-type resonant energy transfer (FRET, also used as Förster resonance energy transfer) is an inverse sixth-power distance-dependent nonradiative energy transfer (Equation 1A) from the exited state ^{1}D of FRET donor luminophore to the exited state ^{1}A of an acceptor luminophore provided that the emission spectrum of the donor luminophore overlaps with the absorption spectrum of the acceptor luminophore and these luminophores are positioned in close proximity [49].

$$A)\ E = \frac{R_0^6}{R_0^6 + r^6} \qquad B)\ E = 1 - \frac{\tau_{DA}}{\tau_D} \qquad C)\ E = 1 - \frac{FI_{DA}}{FI_D}$$

Equation 1. FRET efficiency (E) equations. r is the actual distance between donor and acceptor and R_0 is the Förster distance (where energy transfer is 50%). τ_D and τ_{DA} are the luminescence lifetimes of the free donor and the donor in complex with the acceptor, respectively. FI_D and FI_{DA} are the luminescence intensities of the free donor and the donor in complex with the acceptor, respectively.

The Förster distance (R_0) depends on several factors, including the QY of donor, refractive index of the solution and the spectral overlap integral of donor and acceptor. The typical Förster distance ranges from 1 to 10 nm, and FRET is useful to study biological macromolecules, as this distance is comparable to the diameters of many proteins and thickness of biological membranes. FRET efficiency (E) is defined as proportion of the donor molecules that have transferred excitation state energy to the acceptor molecules, which increases with decrease in the intermolecular distance between the luminophores [50]. In experimental setup, FRET efficiency is calculated based on the change in the luminescence lifetimes (time-resolved mode; Equation 1B) or intensities (steady-state mode; Equation 1C) of the donor in the absence and presence of the acceptor.

A way of discarding the background nanosecond-lived autofluorescence in biochemical and cellular measurements is using rare-earth lanthanides' chelates. As the extinction coefficients of lanthanides are extremely low (less than 10 $M^{-1}cm^{-1}$), lanthanide luminescence can be dramatically enhanced by chelating lanthanide ions with an appropriate organic ligand (antenna effect) [51]. It is proposed that the strongly absorbing chromophore-organic acceptor transfers energy from its T_1 state to the lanthanide ion. Thereby, lanthanides' chelates reveal long decay lifetime (0.5–3 ms) in aqueous solutions and have found widespread use as luminophores in highly sensitive analytical methods, particularly for homogeneous immunoassays [51]. As FRET donors, lanthanide complexes operate at a longer distance (longer R_o) compared to conventional organic fluorophores [47]. However, lanthanide chelates (and metal/organic ligand complexes in general) are prone to dissociation and/or chelate (ligand) exchange, which is of utmost trouble for *in vivo* applications and restricts the choice of chelating agents.

2.4. Inhibitors of PKs

The search for potent and selective PK inhibitor is intensively ongoing in the pharmaceutical industry. There are currently 71 small-molecule kinase inhibitors (SMKIs) approved by the FDA and an additional 16 SMKIs approved by other regulatory agencies [52]. In 1997, Lipinski *et al.* analyzed the structures of approved oral drugs and postulated "The Rule of Five" for the potential lead candidates to proceed to clinical trials [53]. These rules were insightful and helped avoid failures in later stages of drug development, however, new knowledge acquired in two decades has made it clear that many complex diseases need a different approach for successful treatment.

Inhibitors are divided into different classes based on their origin (natural or synthetic), binding character (irreversible or reversible), and positioning of inhibitor in the complex with PK (types I–VI). The classification according to the positioning of the inhibitor in PK complex is summarized in Table 2.

Table 2. Classification of the inhibitors based on the structure of enzyme/inhibitor complex [54]

Type of inhibitor	Binding features	Reversibility (Yes/No)
Type I	Inhibitor binds to the ATP pocket of the active conformation of PK	Yes
Type I1/2	Inhibitor binds to the ATP pocket of the inactive conformation of PK (DFG in)	Yes
Type II	Inhibitor binds to the ATP pocket of the inactive conformation of PK (DFG out)	Yes
Type III	Inhibitor binds to the site next to ATP pocket (allosteric inhibitor)	Yes
Type IV	Inhibitor binds far away from ATP pocket (allosteric inhibitor)	Yes
Type V	Inhibitor occupies two binding sites (bivalent inhibitor)	Yes
Type VI	Inhibitor occupies an active site where it makes covalent bond (covalent inhibitor)	No

Chemical probes are usually described as small molecules that are used to study and manipulate a biological system such as a cell by reversibly binding to and altering the function of a protein within that system [55]. They are complementary to genetic approaches and can rapidly and reversibly inhibit a protein or a protein domain in cells, be used in almost any cell type and reveal temporal features of target inhibition. Inhibitors of PKs can serve as chemical probes. Photoluminescent probes allow the detection of species of interest (proteins) due to a change in their photoluminescence intensity or emission wavelength during the recognition event [56]. This change in photoluminescence can arise due to a variety of factors. Long-lived emissive photoluminescent probes are used in time-resolved bioimaging and biosensing.

2.4.1. Monofunctional inhibitors

Monofunctional inhibitors bind to one pocket only of the protein. Generally, they enable or hinder the binding of natural substrates. Mostly, PK inhibitors target a specific pocket in its structure. There are generic and selective PK inhibitors binding to the conserved ATP pocket of PKs. Staurosporine and 4,5,6,7-tetrabromobenzimidazole are examples of generic PK inhibitors. More selective inhibitors H89 and IP20 for PKAc [57], or SGI-1776 and AZD1208 for PIM kinases [58] have also been developed. These inhibitors have reduced selectivity because they are targeting the conserved ATP pocket of a PK and the lack of specificity sets boundaries to their applications. Besides, intracellular concentration of ATP is 1–10 mM, hence the inhibition potency of an ATP-competitive inhibitor should be relatively high to compete with such a high concentration of ATP [59]. Allosteric inhibitors show more selectivity than aforemen-

tioned inhibitors. A category of specific inhibitors are inhibitory, blocking or neutralizing antibodies [60]. Most of the inhibitory antibodies have been developed for extracellular enzymes [61] due to the poor cellular uptake of antibodies. Many monoclonal antibodies are in pharmaceutical use as drugs. In AGC group of PKs, several inhibitory antibodies have been produced for PKAc, PKG, and PKC [62], [63].

The protein-substrate pocket can also be targeted. Several natural inhibitory proteins play this role of targeting protein-substrate pocket , *e.g.*, PKAr of PKA. In terms of selectivity, the heat-stable natural PK inhibitor (PKI) selectively inhibits PKAc [64], without differentiating between PKAc isozymes. Human PKI has three isoforms: PKIα, PKIβ, and PKIγ. From PKI, several peptide fragments, of which the most potent has low nanomolar affinity to PKAc have been developed [65]. The 5-24 peptide fragment of PKIα ($PKI_{5–24}$) has been extensively used to study the conformational changes in PKAc arising upon binding of PKI and ATP to PKAc. It has been found that almost no entropy change accompanied the $PKI_{5–24}$ binding to PKAc while ATP binding to it caused a negative entropy change, suggesting the PK rigidification [66]. PIM kinases can be potently bound by cell-penetrating nona-arginine peptide with submicromolar affinity [67]. Due to the similarity in recognition sequence of PKAc and PIM kinases, the nona-arginine peptide cannot be considered as a selective inhibitor. Besides, Nair *et al.* have reported the aminopyrimidine derivative JP11646 as a PIM-selective small molecule and the only known ATP non-competitive inhibitor of PIM kinases [68].

The above-mentioned PK inhibitors are reversible, attaching to the PK with non-covalent interactions thus allowing the PK it was inhibiting to start working again once removed (Table 2). Most of the time, irreversible inhibitors are designed to increase their residence time and potency [69]. Ibrutinib is an example of an irreversible inhibitor targeting Cys481 of Bruton tyrosine kinase. It has been used to treat rare lymphoma. Many examples of irreversible inhibitors of Tyr PKs are found in the literature [70]. Recently, a covalent inhibitor of PKAc has been obtained [71]. There are no reports on irreversible inhibitors targeting PIM kinases.

2.4.2. Bifunctional inhibitors

Both ATP-competitive and protein substrate-competitive inhibitors have disadvantages such as problems with selectivity. To overcome these obstacles, bisubstrate inhibitors that covalently connect adenosine analog and peptide mimetic moieties have been developed. Bisubstrate inhibitors consist of two conjugated moieties, each targeted to a different adjacent binding site in the active core of the enzyme [72]. In bisubstrate inhibitors, the free energy of its binding is the sum of the free binding energy of separate moieties with a reduced entropic penalty. In 1991, Ricouart and coworkers reported the first bisubstrate inhibitor against PKs [73].

2.4.2.1. ARC-photo probes

Synthetic middle-sized compounds ARCs are conjugates of adenosine analogs and peptide mimetics. Based on these compounds, supported by extensive structure-affinity studies and X-ray analysis of ARC/PKAcα co-crystals [74]–[76], ARC-inhibitors have been developed. They simultaneously associate with binding sites of both substrates (ATP and substrate protein) and therefore possess good-to-high affinity for PKAcα and several other basophilic PKs. Based on ARC-inhibitors, fluorescent ARC(Fluo) probes were constructed by labeling of ARC-inhibitors with fluorophores at their terminal Lys residue [77]. Often the requested high-affinity fluorescent probes are lacking in the starting phase of a screening campaign. To solve this issue, group-selective ARC(Fluo) probes were previously developed for PKAcα and other basophilic PKs [77]. For testing by biochemical assays with purified proteins, even non-selective inhibitors with known binding modes to a group of PKs have great potential because a single photoluminescent probe constructed from such inhibitors can be used to screen and characterize inhibitors toward the PKs of this group. Later, more selective ARC(Fluo) probes were developed for ROCK [78] and PIM kinases [67].

2.4.2.2. ARC-Lum probes

The adenosine analog moiety of ARC-Lum probes is a heteroaromatic bicyclic or tricyclic fragment with a sulfur or a selenium atom in one of the aromatic rings. The heteroaromatic fragment of an ARC-Lum(−) probe binds to the ATP pocket of the PK where it possesses phosphorescence emission at 500−750 nm upon excitation with a pulse of near-UV radiation [79]. ARC-Lum(Fluo) probes are tandem probes that in addition to the phosphor of ARC-Lum(−) probes incorporate a fluorescent dye with an absorption spectrum overlapping with the phosphorescence spectrum of ARC-Lum(−) probe. The energy of the exited triplet state of the donor is transmitted by resonant energy transfer to the acceptor dye. In complex with the PK, ARC-Lum(Fluo) probes possess enhanced photoluminescent signal compared to ARC-Lum(−) probe with long (τ = 20 – 250 μs in the presence of dissolved molecular oxygen) decay lifetime upon their excitation with a flash of near-UV radiation [79]. ARC-Lum(Fluo) probes are used as tracers for measurements with TGLI or FA readout. In TGLI mode, PK-induced long lifetime luminescence of ARC-Lum(Fluo) probes allows working high concentrations of the probes to shift displacement curves of tested inhibitors away from the tight-binding region to determine their affinity values [80]. TGLI measurement allows discarding the short-lived autofluorescence of cells and bodily fluids.

2.5. Methods for studying inhibitor/PK complexes

2.5.1. Activity and characterization of inhibitors

The PK activity refers to the number of moles of product formed per unit of time. It is expressed in *enzyme units* (U), where 1 U equals the amount of PK that phosphorylates 1 nanomole of a specific substrate within 1 minute at 30 °C [81]. Specific activity is defined as units of activity per milligram of protein. Specific activity is useful for following the purity of an enzyme during purification procedures. The specific activity increases at each step of the purification process. Instead of physiological substrates, a phosphorylatable peptide containing the PK recognition sequence of the substrate can be used [35], [82]. Classically, PK activity was assessed by measuring the adsorption of ^{32}P-labeled phosphorylated substrate on phosphocellulose paper [83]. To avoid the risk related to handling radioactive samples, chromatography methods based on fluorophore-conjugated substrate peptides have been developed [82], [84].

Catalytic activity profiling has also been performed in a high-throughput manner with nanoliter volumes [85]. In these assays, one substrate is taken in excess and time monitoring of phosphorylation rate is carried out (Scheme 1A). The equation describing the resulting pseudo first-order reaction (Scheme 1B) is further simplified by the Michaelis-Menten equation (Scheme 1C), where $V_{max} = k_{cat}[E]_t$ and $K_M = \frac{k_{-1}+k_{cat}}{k_1}$ (Table 1). Each of these assays can be applied for characterization of inhibitors when the assay is performed in the presence of various concentrations of the inhibitor (Scheme 1A). A competitive inhibitor competes with the substrate for binding to the enzyme's active site (Scheme 1A) and its inhibition constant K_i (Scheme 1D) is a measure of its inhibition potency. In increasing the concentration of the competitive substrate, the probability of inhibitor binding decreases and V_{max} will still be reached for a given $[E]_t$ at high enough substrate concentration.

$$\text{A) } EI + S \underset{k_{off}}{\overset{k_{on}}{\leftrightarrows}} I + E + S \underset{k_{-1}}{\overset{k_1}{\rightleftarrows}} ES + I \overset{k_{cat}}{\longrightarrow} E + P + I$$

$$\text{B) } v_0 = \frac{k_{cat}[E]_t[S]}{\frac{k_{-1}+k_{cat}}{k_1} + [S]} \qquad \text{C) } v_0 = \frac{V_{max}[S]}{K_M + [S]} \qquad \text{D) } K_i = \frac{[E][I]}{[EI]}$$

Scheme 1. Inhibition of enzymatic reaction. A) The monosubstrate reaction mechanism in the presence of competitive inhibitor: k_{cat}, the catalytic rate constant of product formation; k_1, the association rate constant; k_{-1}, dissociation rate constant, k_{off}, dissociation rate constant of inhibitor/protein complex; k_{on}, association rate constant of inhibitor/protein complex; E, enzyme; S, substrate; P, product; I, inhibitor. B) Equation for the rate of monosubstrate reaction: v_0, initial velocity; $[E]_t$, the total concentration of enzyme; [S], the concentration of substrate. C) Michaelis-Menten equation: K_M, Michaelis-Menten constant; V_{max}, the maximum rate of substrate conversion. D) Equation of inhibition constant K_i: [E], concentration of free enzyme; [I], concentration of free inhibitor; [EI], concentration of enzyme/inhibitor complex.

Binding assays are a convenient alternative to monitoring substrate phosphorylation in kinetic assays. Instead of using two substrates, binding of the inhibitor to the catalytically active PK is employed. The unlabeled inhibitor can be applied in heterogeneous biosensor assays, such as surface plasmon resonance (SPR) [86]. SPR yields kinetic parameters for the ligand binding along with the value of K_D. Conjugation of the ligand with a fluorophore is required for obtaining a sensitive homogeneous setup. The resulting fluorescent probe is suitable to be used in various fluorescence intensity (FI)-based assays that distinguish between the free probe and probe/enzyme complex. Methods with fluorescence polarization (FP) or FA measurement can be used for determination of both direct binding of the probe to the PK and displacement of the probe from the complex with a PK by an inhibitor [77], [87]. FP and FA are interchangeable quantities, while the usage of FA is preferred as it accounts for total FI (Equation 2).

$$\text{A)}\ p = \frac{I_{\parallel} - I_{\perp}}{I_{\parallel} + I_{\perp}} \qquad \text{B)}\ r = \frac{I_{\parallel} - I_{\perp}}{I_{\parallel} + 2I_{\perp}}$$

Equation 2. p, polarization; $I_{\parallel}$, emission intensity parallel to plane-polarized incident light; $I_{\perp}$, emission intensity perpendicular to plane-polarized incident light; r, anisotropy.

FP measurements function based on depolarization of the emission intensity of a fluorophore when excited with plane-polarized light. The degree of depolarization is a function of molecular properties, specifically the Brownian molecular rotation, and hence can serve as an effective sensor of molecular complex size. In the classical assay format, it is impossible to characterize binders whose affinity toward the target protein is higher than that of the fluorescent probe. However, in using ARC-Lum(Fluo) probes, measurable IC_{50} values may be substantially shifted by the application of a significant excess of probes, compared with the target protein, that emit a negligible signal in their free TGLI detection mode [79]. Finally, many companies have developed FP-based assay kits: BellBrook's Transcreener™, DiscoveRx's HitHunter™, Invitrogen's Far-Red PolarScreen™, Millipore's KinEASE™, and Molecular Devices'IMAP™.

2.5.2. Thermodynamics of inhibitor/PK binding

The first requirement of a promising lead molecule is its sufficient affinity toward its target. This affinity is expressed as equilibrium dissociation constant (K_D) of the complex between target protein (P) and inhibitor (I) (Equation 3).

A) $P + I \leftrightharpoons PI$ B) $K_D = \frac{[P][I]}{[PI]}$ C) $\ln K_D = \frac{\Delta G_B^\circ}{RT} = \frac{\Delta H_B^\circ - T\Delta S_B^\circ}{RT}$

Equation 3. Protein-inhibitor interaction characterization. A) Chemical equation of protein and inhibitor binding interaction. B) K_D, equilibrium dissociation constant of the complex P/I: [P], equilibrium concentration of free protein; [I], equilibrium concentration of free inhibitor; [PI], equilibrium concentration of protein/inhibitor complex. C) ΔG_B°, standard free energy change of the binding; R, ideal gas constant; T, absolute temperature; ΔH_B°, standard enthalpy change of binding; ΔS_B°, standard entropy change of binding.

Protein-inhibitor interactions are accompanied with the changes in the free energy (ΔG_B°), enthalpy (ΔH_B°), entropy (ΔS_B°), and heat capacity (ΔC_p) of the system [88]. When the protein-inhibitor interaction is strong, the K_D value of their complex is small. K_D is exponentially proportional to standard free energy change of binding, ΔG_B° (Equation 3C) that comprises both enthalpic (ΔH_B°) and entropic (ΔS_B°) changes upon binding. Minimization of ΔG_B°, thus decrease of K_D is possible by strengthening interactions (negative ΔH_B°) or inflicting disorder at the protein-binding interface (positive ΔS_B°) upon binding. Strong inhibitors make qualitative electrostatic or hydrophobic interactions with their protein targets. The thermodynamic characterization of ligand–protein binding is most often performed with isothermal titration calorimetry measurements [89]. They directly provide full thermodynamic profile of the binding. Valuable insight into the binding process can be obtained by combined structural and thermodynamic analyses of a set of related complexes. These analyses are able to reveal how various effects like the water mediated ligand–protein binding, the displacement or trapping of water molecules upon ligand binding, and the interplay between hydrogen-bonding and hydrophobic contacts influence the thermodynamic balance of binding [88], [89].

Inhibitor–protein binding in water is a complex process with various competing enthalpic and entropic contributions. The basic challenge in affinity optimizations can be formulated as to overcome enthalpy–entropy compensation to achieve decreased K_D. Optimizing both $\Delta H_B^\circ$and ΔS_B° is frequently conflicting. Employing an enthalpic optimization strategy may be beneficial in early-medium stages in the drug-discovery process because it will determine the drug quality of the compound, and entropic optimization can still be performed in late-stage optimization in making inhibitors more rigidified. This rigidification can also alter selectivity among PKs [90]. Besides, rigidification can help for better positioning the warhead moiety of covalent inhibitors in the complex with PKs [91].

2.5.3. Immunosorbent assays

Radioimmunoassays were first described in 1959 as a method to study the physiology of peptide hormone insulin. In the quest for an alternative method not using radioactivity measurement, the enzyme-linked immunosorbent assay (ELISA) was introduced in 1970s [92]. ELISA is a widely used diagnostic tool in medicine taking advantage of immunoaffinity purification of analytes (hormones, proteins, and antibodies). Additionally, in affinity chromatography, bound proteins can be selectively released using a competitive ligand. The major advantage of ELISA is the use of washing steps, which allow removing the unbound material. Hence, because ELISA is a heterogeneous method with several washing steps (specialized plate washers for improved repeatability are used) and reagent incubations, such method tends to be time-, cost-, and labor-ineffective. Further, there is a risk of losing the material specifically bound on the solid surface. Therefore, the sensitivity of ELISA may suffer from various intervening steps and heterogeneity of the sample (*e.g.*, blood). Besides, an assay performed with microscopic beads is typically 1000-fold more sensitive than the conventional ELISA assays [93]. Finally, a classical ELISA assay requires the application of two orthogonal antibodies of the analyte, which are not always easy to obtain [94].

Protein microarrays, also known as protein chips, are miniaturized and parallel assay systems that contain small amounts of purified proteins. Protein microarrays have been applied for the analysis of antigen–antibody or protein–protein interactions [95]. Protein microarrays are made of immobilized molecules (proteins, peptides, or small organic molecules) addressed on glass or polymer slides. In functional protein microarrays, the analyte must retain activity and remain stable during the experimental steps. Compared with traditional assays, the protein chip-based assays have several advantages, *i.e.*, reduction in biological sample volume, high sensitivity, ease of performance, and large data generation [95]. However, microarray immunoassays have kinetic limitations, which may be slowed down as much as hundreds of times compared with the solution kinetics [96].

2.5.4. X-ray crystallographic studies and ligand binding modes

Apart from using X-ray crystallography, binding modes of inhibitors in proteins can be determined in solution by nuclear magnetic resonance (NMR) [97]. As of 22 July 2021, 88% of the structures in Protein Data Bank (PDB) were obtained by X-ray diffraction analysis but 7.4% of structures were determined by solution NMR. A search of the PDB for gene name "*PIM1*" on 22 July 2021, identified 167 PIM-1 crystal structures compared to 329 PKAcα crystal structures with gene name "*PRKACA*" being searched on the same day. These numbers account also for mutated kinases of PIM-1 and PKAcα, and holoenzymes of PKA. No results of a crystallographic study on PKAcβ and PIM-3

have been published up to date. Furthermore, protein crystals contain a large amount of solvent (water content 40-60%), allowing relatively free diffusion of small compounds through the crystal, allowing keeping the protein in the native state. Below, we compared the co-crystal structures of PIM-1 and PKAcα with AMP-PNP (PDB 1XR1) and ATP (PDB 1ATP), respectively (Figure 3).

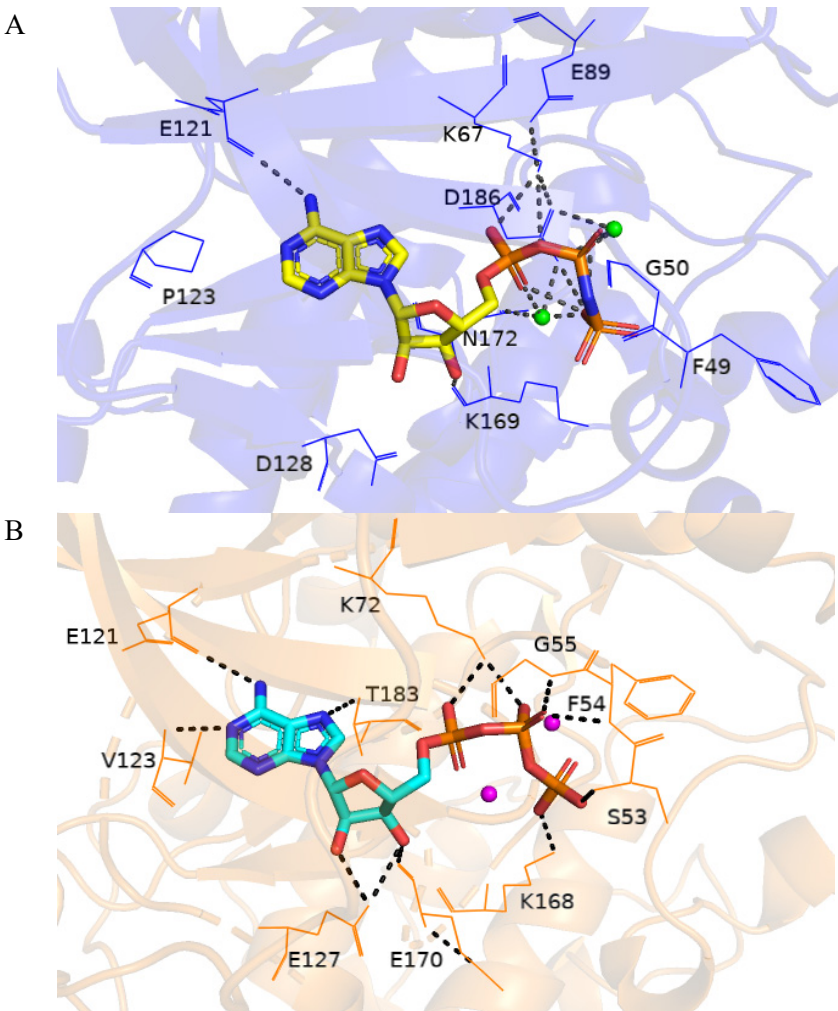

Figure 3. Comparison of interactions of nucleotide molecules bound to ATP-site of PIM-1 or PKAcα. A) Co-crystal structure of the kinase domain of PIM-1 with AMP-PNP (PDB 1XR1). PK is shown as blue cartoon; B) Co-crystal structure of PKAcα with ATP (PDB 1ATP). PK is shown as orange cartoon. Residues of PKs forming interactions with the co-crystallized small molecules are shown as lines and are labeled; hydrogen bonds are shown as black dotted lines. Mg^{2+}-ions are shown as green spheres. Mn^{2+}-ions are shown as magenta spheres.

Like in PKAcα, the ATP-binding pocket of PIM-1 is a narrow groove between the C- and N-lobes. The K_M values of ATP for PIM-1 and PKAcα are given in Table 1. The adenine ring of ATP is bound to the hydrophobic cleft locating between the lobes. The amino group of adenine ring gives a H-bond with Glu121 of both PIM-1 and PKAcα and its nitrogen atom at position 1 gives a H-bond with Val123 in PKAcα while the corresponding Pro123 in PIM-1 does not give such interaction (Pro residue cannot act as a hydrogen bond donor) (Figure 3). The hydroxyl groups of ribose ring do not interact with PIM-1 residues while they interact with PKAcα (Glu127 and Glu170 with 3'-hydroxyl and 2'-hydroxyl groups, respectively). Furthermore, α-phosphate of the nucleotide is coordinated via the conserved Lys67 residue in PIM-1 (Lys72 in PKA) and, at the same time, Lys67 forms the salt bridge with Glu89 of αC-helix (the latter is a hallmark of active kinase) [98]. Next, in Ser/Thr PKs, γ-phosphate forms a charge reinforced hydrogen bond with highly conserved Lys (Lys168 in PKA, which interacts with γ-phosphate of ATP, aspartate of HRD, activation loop and substrate peptide), and this interaction is required for phosphoryl transfer. In PIM-1, the conserved Lys169 does not interact with γ-phosphate of AMP-PNP (Figure 3) and the phosphoryl-transfer role is fulfilled by Asp167 [98]. In addition to the previously mentioned polar contacts, the nucleotide ring systems are stabilized by hydrophobic and π-π interactions with AAs of PIM-1 (*e.g.*, Leu44, Val52, Ala65, Leu174, Ile185) [98] and AAs of PKAcα (*e.g.*, Leu49, Val57, Val104, Met120, Tyr122, Leu173) [99]. The binding modes of substrate peptides in PIM-1 and PKAcα are quite similar [98].

3. AIMS OF THE STUDY

This study was focused on the construction of inhibitors and fluorescent probes as research tools for analysis of PKs in biochemical solutions, cell lysates, and living cells. These were the main tasks addressed in the present thesis:

- Application of protein binding-responsive ARC-Lum(Fluo) probes for screening and characterization of inhibitory antibodies for specific regulation of activity of PK PKAcα1.
- Development of a photoluminescent assay for analysis of a new protein target PKAcβ1, involved in CS, and construction and characterization of wild-type sparing inhibitors for regulation of activity of the mutated protein S54L-PKAcβ1.
- Construction of inhibitors with simplified chemical structure for PK PIM-1, guided by results of the first X-ray analyses of crystals of complexes of ARC-inhibitors and the protein. Application of the new fluorescent probes, inhibitors labeled with fluorescent dyes for microscopy experiments in living cells.
- Development of a sandwich-type assay for specific determination of the cancer biomarker PK PIM-2 in biological solutions, based on the cooperative use of a new ARC-probe and specific monoclonal PIM-2 antibody.

4. METHODS

4.1. Competitiveness of mAb(D38C6) and ARC for binding to PKAcα1

The assay buffer contained HEPES hemisodium salt (Sigma) (pH 7.4, 50 mM), NaCl (Riedel-de Haën) (150 mM), and Tween-20® (Sigma) (0.005%) in the presence or absence of ARC-1415 (1 μM), in final volumes of 20 μL in wells of 384-well low-binding surface microtiter plates (Corning, code 4514), read with the PHERAstar microplate reader (BMG Labtech). The assay was performed by titrating fixed concentration of the complex of europium chelated streptavidin (2 nM) and biotinylated PKAcα1 (1.5 nM) with Alexa Fluor 647-labeled mAb(D38C6) and preincubated at 30 °C for 30 min. Measurements were conducted in duplicate, for which standard deviation is depicted. GraphPad Prism version 5.04 (GraphPad Software, Inc.) was used for data visualization.

4.2. Biochemical assays with measurement of FA or TGLI

Optical FA measurement modules [ex. 540(20) nm, em. 590(20) nm and 590(20) nm] and [ex. 590(50) nm, em. 675(50) nm and 675(50) nm] were used for orange-fluorescent-dye-labeled and red-fluorescent-dye-labeled probes, respectively, in assays with the PHERAstar microplate reader. TGLI measurement modules [ex. 330(60) nm, em. 590(50) nm] and [ex. 330(60) nm, em. 675(50) nm] were used for orange-fluorescent-dye-labeled and red-fluorescent-dye-labeled probes, respectively, in assays with the same instrument. The measurement solutions (20 μL volumes) were prepared in black 384-well low-binding surface microtiter plates (Corning, code 4514) and incubated at 30 °C for 20 min before the measurements. The assay buffer contained HEPES hemisodium salt (pH 7.4, 50 mM), NaCl (150 mM), dithiothreitol (Sigma) (5 mM), bovine serum albumin (Sigma) (0.5 mg/mL), and Tween-20® (0.005%). GraphPad Prism version 5.04 (GraphPad Software, Inc.) was used for data analysis with FA [77] or TGLI readout [100].

The luminescence decay curves were fitted to the Equation 4.

$$I = \left(I_0 - I_{bg}\right) \cdot e^{-t/\tau} + I_{bg}$$

Equation 4. Fitting luminescence decay data. I is the intensity of the luminescence signal measured at time t, I_0 is the intensity of the luminescence signal at t = 0, I_{bg} is the intensity of the signal of the background and τ is the luminescence lifetime.

4.3. Co-crystallization, diffraction data collection, and structure determination

Final concentrations of PIM-1 and the inhibitors in crystallization solutions were 0.1 mM and 1 mM, respectively. Crystals of complexes were grown using the sitting-drop vapor-diffusion method at 4 °C with a reservoir solution listed in **Paper III, Table S1**. Diffraction data were collected at Diamond Light Source, processed, and scaled with XDS [101] and AIMLESS [102], respectively. Structures were solved by molecular replacement using Phaser [103] and the coordinates of crystal structure of PIM-1 (PDB 2J2I; [104]) as the search model. Model rebuilding and structure refinement were performed in COOT [105] and REFMAC5 [106], respectively. Data collection and refinement statistics are summarized in **Paper III, Table S1**.

4.4. Solid phase peptide synthesis

Peptide fragments were prepared by using traditional Fmoc solid phase peptide synthesis on Rink amide MBHA resin [67], [107]. Protected amino acids (3 eq.) were dissolved in DMF and activated with HBTU/HOBt (2.85 eq. each) and NMM (6 eq.) in DMF. After 3 min, the coupling solutions were added to the resin and shaken at room temperature (RT) for 40–60 min at RT. The completion of each coupling step was monitored with the Kaiser test. Removal of N-terminal Fmoc-group was performed with 20% piperidine solution in DMF (20 min). After each step, the resin was washed 5 times with DMF.

The adenosine analog fragments of ARCs are not commercially available and smaller equivalents compared to AA were used to save the reagents. Carboxylic-acid-functional fragments (1.5 eq.) were mixed with HBTU (2.85 eq.), HOBt (2.85 eq.) and DIPEA (6 eq.) in DMF and added to the resin (1 eq.), and the reaction mixtures were shaken at RT for 60 min. Chloromethyl-functional fragments (1.5 eq.) in DMF and DIPEA (6 eq.) were added to N-terminal amino group of the corresponding peptides on the resin (1 eq.) and stirred slowly at 60 °C for 8 h. After getting the entire designed compound ready on the resin, the cleavage was carried out using the mixture of TFA/ H2O/TIPS (90/5/5) for 3 h. The product was collected and evaporated to dryness in vacuo. Trituration with methyl-tert-butyl ether was followed by another evaporation in vacuo. The products were purified by reversed phase HPLC using a C18 column.

4.5. Surface sandwich assay for PIM-2 measurement

The composition of the assay buffer was as follows: HEPES (50 mM), NaCl (150 mM), Tween-20® (0.005%). The Pierce streptavidin-coated microtiter plate (#15407) was used for the preparation of the ARC-affinity surface. ARC-2073 in 10 mM phosphate buffer (pH = 7.0; 80 nM, 50 µL) was added to the wells and incubated for 60 min at RT under constant shaking at 300 rpm. All the following incubations steps in the assay were performed in the same conditions. After each incubation step, the wells were washed with assay buffer (100 µL) for 10 s at RT under constant shaking at 300 rpm. All the following washing procedures were performed similarly. Thereafter, PIM-2 in assay buffer (50 µL) was added to the ARC-affinity wells, incubated, and removed. Then, primary antibody D1D2 (1.7 nM, 50 µL) in assay buffer was incubated in the wells and removed. Finally, europium chelate-labeled secondary antibody (G0506) (2.2 nM, 50 µL) was incubated in the wells and removed from them. The wells were washed, dried under fume hood for 10 min and TGLI was measured on their surfaces with the PHERAstar microplate reader. GraphPad Prism v. 5.04 was used for data analysis. The limit of quantification (LoQ) was calculated based on the standard deviation of the calibration curve (SD) and the slope of the calibration curve (S) using the equation $LoQ = 10 \times SD/S$.

5. SUMMARY OF RESULTS AND DISCUSSIONS

5.1. Conformational rearrangements in PKAc (Paper I and unpublished data)

5.1.1. Discovery of inhibitory properties of the antibody mAb(D38C6) against PKAcα1

Therapeutic antibodies have been used in the treatment of cancer, autoimmunity, and inflammatory diseases [108]. Research with plasma proteases has demonstrated the potential of inhibitory antibodies for drug development [61]. Besides, the neutralizing monoclonal antibody against plasma kallikrein, lanadelumab has been approved for treating hereditary angioedema since 2 years [60]. Several inhibitory antibodies against PKs of the AGC group have been reported [62] and strategies for their cellular uptake have still to be developed. ARCs are bisubstrate inhibitors binding to both substrate pockets of PKAcα1 and other PKs [75]–[77]. Hereinafter, the isoform PKAcα1 will be denoted PKAcα.

In attempt to establish the formation of a three-component complex by detection of FRET between the PKAcα active site-binding ARC-Lum(Fluo) photoluminescent probe and Alexa Fluor 647-labeled antibody mAb(D38C6) [mAb(D38C6)-AF647] against PKAcα (ARC/PKAc/Ab), we discovered that mAb(D38C6)-AF647 displaced the probe from its complex with PKAcα (**Paper I**, Figure 1). The same behavior was observed in an alternative assay (Figure 4). The assay components were europium chelate-labeled streptavidin, biotinylated PKAcα and mAb(D38C6)-AF647. Under this format, FRET was detected between the europium chelate and Alexa Fluor 647 with an efficiency of 83% after excitation with near-UV radiation. The biotinylation of PKAcα at its N-terminus had no effect on its binding to mAb(D38C6). Application of the competitive ARC-inhibitor ARC-1415 (**Paper III**, Figure 1) led to cessation of FRET between the FRET partners because of displacement of mAb(D38C6)-AF647 from its complex with PKAcα (Figure 4).

Competitiveness in binding of mAb(D38C6) and ARC-probe to PKAcα points to the partially overlapping “epitopes” of the two binders [109]. In other words, the association of PKAcα with ARC or mAb(D38C6) leads it to adopt two different conformations. ARCs and mAb(D38C6) are bound to the active and inactive conformation of PKAcα, respectively. mAb(D38C6) binds to the kinase possessing non-ordered conformation of the C-tail. Contrarily to mAb(D38C6), association with ATP-pocket binding inhibitors or ATP causes PKAcα to adopt an active conformation: C-terminal tail is ordered and Phe327 residue of PKAcα’s AST region takes part in formation of the ATP pocket [110]. Phe327 is an AA in the linear peptide epitope of mAb(D38C6) (raised in rabbit against a peptide sequence around Ser326) and it translocates extensively when PKAcα is passing from its active conformation to the inactive conformation (**Paper I**, Figure 7). mAb(D38C6) inhibited PKAcα-catalyzed reaction between ATP and substrate peptide kemptide with high inhibitory

potency (**Paper I**, Figure 2). The inhibitory potency of mAb(D38C6) was calculated by the Cheng-Prusoff equation using K_M value of 17 µM for ATP (Table 1). Its inhibitory potency (K_i = 2.4 nM) was close to its binding affinity, measured *via* displacement of the probe (K_D = 1.2 nM). Furthermore, the IC_{50} of mAb(D38C6) increased approximately 10-fold when increasing the ATP concentration 10-fold in a PK inhibition assay (**Paper I**, Figure S3). Using a genetically engineered variant of a cAMP-sensor [76], the non-disruption of PKAcα/PKArIIβ complex was confirmed when mAb(D38C6) was applied as an ATP-competitive PKAcα inhibitor.

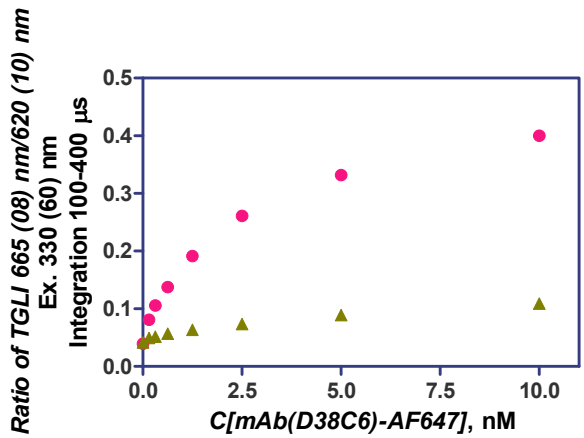

Figure 4. Competitiveness between mAb(D38C6) and ARC-1415 for the binding to PKAcα. FRET between europium chelate-labeled streptavidin (2 nM) interacting with biotinylated PKAcα (1.5 nM), and mAb(D38C6)-AF647, without (pink ●) and with (green ▲) competitive compound ARC-1415 (1 µM) was measured. Measurement was in duplicate, and variance was expressed as standard deviation.

Although mAb(D38C6) possesses outstanding inhibitory properties, its use in cellular experiments is not possible due to its cellular impenetrability and low stability of mAb-s in cellular environment, but also due to its competitiveness with ATP present in cells at millimolar concentrations [59]. However, the use of mAb(D38C6) is possible in biochemical studies and for measurements in cell lysates and bodily fluids [93]. The specific and sensitive AbARC assay was developed to determine PKAcα in complicated biological solutions (**section 5.4.1** of this thesis). The majority of PKs lack specific inhibitors; therefore, availability of a novel specific research tool has great value for establishment of the role of a PKAc isozyme in signaling cascades. For PKAc, a thermostable natural inhibitory protein PKI exists [64], [111], but even this inhibitor does not differentiate among PKAc isozymes. Inhibitory antibody mAb(D38C6) with PKAcα isozyme specificity (**Paper I**, Figure S4) could be useful for deleting the activity of this isozyme in lysates to establish the role of this enzyme as the regu-

lator of protein phosphorylation balances [26]. Such specific inhibitor can also be applied to study the non-redundancy in functions of PKAc isozymes [112].

In case of other PKs of the AGC group, highly selective inhibitors (like PKI for PKAc) are missing. However, several PKs of this group also possess Phe residue in the C-tail of the protein that takes part in the formation of the ATP pocket in the active conformation of the kinase [113]. Therefore, the approach that was tested for mAb(D38C6) might work with other AGC kinases. As ARC-Lum(Fluo) probes possess high affinity toward many AGC kinases [79], these probes that have demonstrated their usefulness for screening and characterization of monoclonal antibodies against PKAcα would greatly support studies with other AGC kinases. A similar competitiveness phenomenon has been reported before [61], showing that N-TIMP-2, an endogenous inhibitor of proteinase MMP-9 causes the dissociation of the complex of the inhibitory monoclonal antibody Fab L13 and catalytic domain of MMP-9. The epitope of the latter antibody is restructured and masked by N-TIMP-2. Additionally, other examples of modulation of the activity of various proteins with antibodies by orthosteric, allosteric, and parasteric mechanisms have been described [62], [109], [114].

5.1.2. TGL properties of ARC-1085 and ARC-1086 in complex with PKAcβ1 and S54L-PKAcβ1

L205R mutation in PKAcα, found in 67% of patients suffering from CS, leads to loss of binding of PKAcα with PKAr [15]. Recently, a somatic mutation was identified in the *PRKACB* gene, encoding PKAcβ1, in a cortisol producing adenoma from a female patient with severe CS [16]. This mutation is a replacement of Ser54 (AA residue possessing a small and hydrophilic side chain) with Leu (AA with a middle-sized and hydrophobic side chain) leading to alteration in the structure of GRL (amino acids 48–57), a flexible peptide motif that plays a crucial role in the regulation of activity of the enzyme. S54L-PKAcβ1 is hyperactive at basal level. In the following, PKAcβ1 and S54L-PKAcβ1 will be denoted PKAcβ and S54L-PKAcβ, respectively.

ARC-1085 and ARC-1086 are both probes with the same thiophene-comprising adenosine analog moiety but possessing a different location of the fluorescent dye Alexa Fluor 647 (AF647) in their structures (Scheme 2). In ARC-1085, AF647 is attached to the C-terminal D-Lys residue. In ARC-1086, AF647 is attached to the chiral spacer D-Lys residue. The location of the FRET acceptor AF647 was modified in probes when originally studying protein-induced long-lifetime luminescence of ARC-Lum(Fluo) probes [79]. It was hypothesized that location of the acceptor AF647 would affect the FRET in PKAcβ and its mutant PK. If ARC-1085 and ARC-1086 were compared for their TGL properties in complex with PKAcβ and S54L-PKAcβ, both ARC-Lum(Fluo) probes emitted microsecond-scale luminescence upon excitation with near-UV radiation if in complex with the kinases (Table 3). Free probes revealed negligible long-lifetime signals.

Table 3. Relative zero-timepoint luminescence intensity I_0 (I_0 = 1 for ARC-1085 in complex with PKAcβ) and luminescence decay lifetime τ_{DA} (μs) for ARC-Lum(Fluo) probes in complex with PKs. Final concentrations of the probe of 1 nM and PK of 75 nM were used

	PKAcβ			S54L-PKAcβ		
Compound	I_o	τ_{DA}, μs	K_D, nM	I_o	τ_{DA}, μs	K_D, nM
ARC-1085	1.00±0.01	136±4	0.06±0.01	0.89±0.01	137±4	0.064±0.010
ARC-1086	2.91±0.03	75±3	6.0±0.3	2.07±0.02	84±3	6.0±0.3

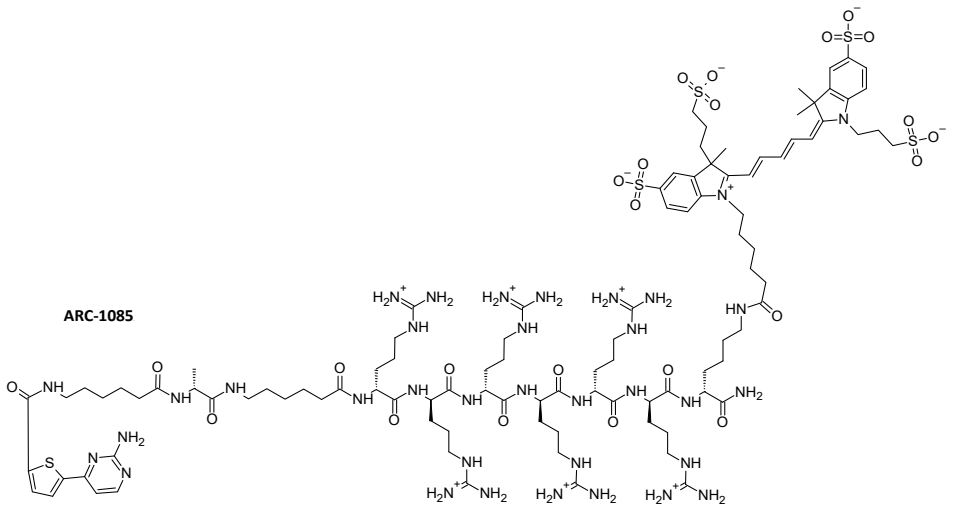

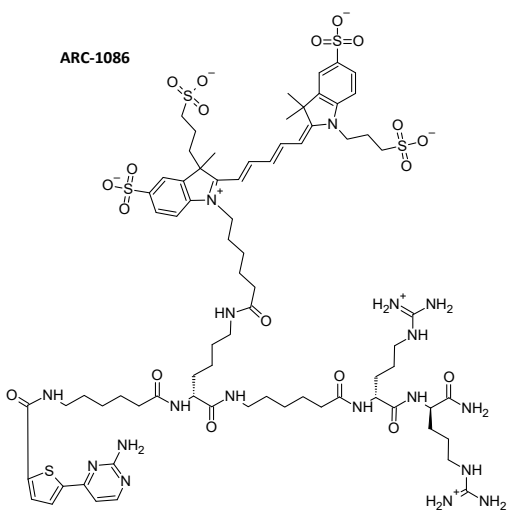

Scheme 2. Structures of ARC-1085 and ARC-1086

Relative zero-timepoint luminescence intensities (I_0) of complexes with PKAcβ were slightly higher than those with S54L-PKAcβ (Table 3). Values of luminescence decay lifetime of ARC-1085 in complexes with both proteins were similar. As expected, ARC-1086 revealed shorter luminescence decay lifetime values and higher I_0 values compared to ARC-1085 if in complex with PKAcβ and S54L-PKAcβ due to shorter distance between the FRET donor and acceptor in ARC-1086. Values of luminescence decay lifetime for ARC-1086 in complex with PKAcβ and S54L-PKAcβ were 75 μs and 84 μs, respectively (Table 3). The difference in I_0 and lifetime values indicates the difference in binding modes of PKAcβ and S54L-PKAcβ, although having the same affinity to ARC-probes (Table 3). Each binding mode leads to a particular rigidified double complex [115] protecting the probe differently from molecular oxygen quenching [116]. Finally, it can be argued that S54L substitution introduces a slightly bigger hydrophobic residue at the tip of GRL of PKAcβ, which makes it adopt a more open conformation and position the acceptor dye AF647 further from the FRET donor in S54L-PKAcβ complexes.

5.2. Development of wild-type-sparing inhibitors for S54L-PKAcβ (Paper II and unpublished data)

Potent inhibitors with wild-type – sparing capability (WC) provide a great tool to discriminate between PKAcβ and S54L-PKAcβ in biomedical studies. WC is the capacity of the compound to effectively inhibit the phosphorylation catalyzed by S54L-PKAcβ and to be less effective against wild-type (wt) PKAcβ. The study on novel protein targets PKAcβ and S54L-PKAcβ was started with working out a photoluminescence-based binding/displacement assay for screening and characterization of inhibitors with using ARC-probes. ARCs are conjugates of adenosine analog moiety and peptide mimetic moiety tethered by linkers. ARCs of the last generation have a chiral spacer between the linkers for proper positioning of the peptide mimetic moiety into the protein substrate pocket of PKAcα [72]. The amide group of the chiral spacer makes a H-bond with the hydroxyl group of Ser54 in PKAcα [75]. We had hypothesized that the disruption of this interaction would help in increasing the index of WC (IWC) of the compounds. IWC of a compound is defined as the ratio of K_D value of the wt PK to K_D of the mutated PK. Furthermore, ARC-precursors are a fragment of ARC comprising only the adenosine analog moiety, the first linker, and the chiral spacer.

We had previously constructed high-affinity fluorescent probes based on ARC inhibitors possessing K_D values in picomolar and nanomolar range for PKAcα and other basophilic PKs. PKAcα and PKAcβ possess great structural similarity, therefore some probes were tested with wt PKAcβ and S54L-PKAcβ in a biochemical assay. Titration of fluorescent probes ARC-583, ARC-669, and ARC-1085 (**Paper II**, Table I and **Paper II**, Table SI) with the purified recombinant S54L-PKAcβ revealed K_D values of 1.76 nM, 233 pM, and 64 pM

for their complexes with the protein, respectively (**Paper II**, Table I), whereas affinity of the probes toward wt PKAcβ was even higher (ARC-583, K_D of 160 pM; ARC-669, K_D of 55 pM; ARC-1085, K_D of 60 pM). The probe ARC-669 possesses higher IWC value than ARC-583. ARC-1085 possesses higher IWC value than ARC-669 (**Paper II**, Table I). These ARC-probes were successfully applied for the characterization of inhibitors against PKAcβ and S54L-PKAcβ. Moreover, we described the first wild-type – sparing inhibitors of S54L-PKAcβ.

The chirality of the inhibitors **1**, **2**, **3**, and **4** slightly affected their IWC (Table 4). The protein targets were able to bind inhibitors that contained either a L- or D-amino acid, whereas the conjugates comprising a D-amino acid residue (Table 4, compounds **1** and **3**) possessed higher affinity than their L-amino acid incorporating counterparts (Table 4, compounds **2** and **4**). This trend in the structure-activity profile of ARCs and ARC-precursors with PKAcβ and S54L-PKAcβ is like the trend previously reported for ARCs with basophilic PKs PKAcα, ROCK-II, and PKGIα [77], [107]. The introduction of the chiral spacer 4-benzoylphenylalanine comprising a bulky and hydrophobic side chain (compounds **3** and **4**) led to higher IWC values than the use of D- and L-Lys spacers (compounds **1** or **2**). Next, variation of the length of α,ω-AA first linker of ARC-precursors with another chiral spacer, Arginine, did not lead to an enhancement of IWC (compounds **5**-**7**). They possessed constant IWC of 0.2. Though, prolonging the first linker led to increased affinity for S54L-PKAcβ and its wt protein (Table 4).

The amide group of the chiral spacer in compound **7** was methylated at the amino group yielding compound **8**. It revealed 2-fold better IWC value than compound **7,** as expected. The control compound **9**, without methylation of the target amino group, revealed the same IWC like compound **8** with a 3-fold better affinity toward both PKAcβ and S54L-PKAcβ. Compound **10** does not comprise a chiral spacer, but it comprises an amide group between the linkers, thus it still contains a H-bond acceptor group in proximity of Ser54. The compound has a low IWC value of 0.3. Use of D-Trp as the chiral spacer yielded moderately wild-type−sparing ARC inhibitors (Table 4). Compounds **11** and **12** revealed similar IWC values of 5.7 ± 1.3 and 4.5 ± 0.7, respectively; Table 4. Compound **11** (**Paper II**, Figure 1) had K_D values of 29 nM and 5 nM toward PKAcβ and S54L-PKAcβ, respectively (Table 4). However, prolonging compound **12** into the protein substrate pocket (yielding compound **13**) worsened 6.4-fold its IWC, whereas affinity of compound **13** was increased to two-digit picomolar range (Table 4). The worsening of IWC is explained by the flexibility of both binding partners, PK and ARC: small changes in the structure of ARC can lead to great changes in the 3-dimensional structure of the complexed PK [75]. It is in line with conformational rearrangement studied with TGLI measurements in **section 5.1.2** of this thesis. Prospectively, D-Trp residue can be further derivatized in the quest for a more wild-type−sparing ARC-precursor than compound **11**.

Table 4. Structures, dissociation constants (K_D), and IWC of the compounds **1**–**13**

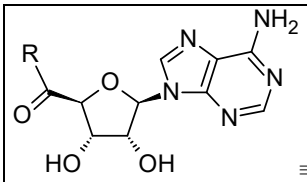

≡ Adc

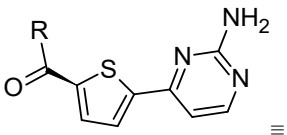

≡ AMTH

Com-pound #	Adenosine analog moiety	First linker	Chiral spacer	Second linker	Peptide mimetic moiety	K_D, nM (SE)		*IWC*†
						PKAcβ	S54L-PKAcβ	
1	Adc	Ahx	**D-Lys**	Ahx	$(D\text{-}Arg)_2\text{-}NH_2$	3.6 (0.1)	20.6 (1.3)	0.2
2	Adc	Ahx	**L-Lys**	Ahx	$(D\text{-}Arg)_2\text{-}NH_2$	227.6 (16.8)	522.9 (45.9)	0.4
3	Adc	Ahx	**D-Phe(Bz)-NH_2**	**---**	---	252.3 (10.6)	367 (26.8)	0.7
4	Adc	Ahx	**L-Phe(Bz)-NH_2**	**---**	---	3,817 (382)	3,262 (262)	1.2
5	AMTH	**Aoc**	D-Arg-NH_2	---	---	2.3 (0.3)	9.9 (0.9)	0.2
6	AMTH	**Ahp**	D-Arg-NH_2	---	---	4.6 (0.5)	19.2 (2.0)	0.2
7	AMTH	**Ahx**	D-Arg-NH_2	---	---	15.1 (2.0)	74.2 (7.7)	0.2
8	AMTH	**Ahx**	D-Arg	**Sar**-NH_2	---	182.6 (12)	494.3 (32)	0.4
9	AMTH	**Ahx**	D-Arg	**Gly**-NH_2	---	59.6 (2.7)	161.7 (12)	0.4
10	Adc	Ahx	**---**	Ahx	$(D\text{-}Arg)_2\text{-}NH_2$	26.1 (3.0)	86.9 (8.6)	0.3
11	AMTH	**Aoc**	D-Trp-NH_2	---	---	28.7 (1.8)	5.0 (0.8)	5.7
12	AMTH	**Ahx**	D-Trp-NH_2	---	---	222.9 (12.4)	49.9 (4.7)	4.5
13	AMTH	**Ahx**	D-Trp	**Ahx**	**$(D\text{-}Arg)_6$-D-Lys**-NH_2	0.013 (0.002)	0.019 (0.002)	0.7

Adc – adenosine-4′-dehydroxymethyl-4′-carboxylic acid moiety; AMTH – 5-(2-aminopyrimidin-4-yl)-thiophene-2-carboxylic acid moiety; Ahx – 6-aminohexanoic acid moiety; Ahp – 7-aminoheptanoic acid moiety; Aoc – 8-aminooctanoic acid moiety; Phe(Bz) – para-benzoylphenylalanine; Sar – sarcosine. † – IWC = K_D(PKAcβ)/ K_D(S54L-PKAcβ). Measurements were performed in triplicate and the data variance was characterized with the standard error (SE).

A generic inhibitor of PKs, staurosporine turned out to be 17-fold more wild-type sparing than PKAc-selective inhibitor H89 (Table 5). H89 does not induce such conformational changes to PKAcα as staurosporine [117]. Inhibitor H89

has been used in several biomedical studies involving PKAcβ [26], [114], [118] but its affinity to the kinase has not been disclosed. We were the first to report a K_D value of 1.0 nM for H89 in complex with PKAcβ. A comparison of our FA-based assay to ADP-Glo™ kinase assay revealed a similar dissociation constant for staurosporine to PKAcβ (K_D = 0.71 nM *vs* K_i = 0.67 nM). The WC of inhibitors previously developed to target other basophilic PKs were determined too. A derivative of staurosporine and PKC-selective inhibitor, BIM VIII revealed very low IWC (smaller than 0.03), which is even lower than that of H89 (IWC of 0.07). A PIM-elective inhibitor, SGI-1776 revealed single-digit micromolar affinity to both PKAcβ and S54L-PKAcβ (Table 5) with a good WC (IWC = 0.7). GSK690693, a pan-AKT inhibitor is as wild-type sparing as SGI-1776 with nanomolar affinity to both PKAcβ and S54L-PKAcβ (Table 5). GSK690693 induces conformational changes to AKT PKs [119], which are closely related to PKAcα. Finally, among tested ATP-competitive inhibitors, staurosporine turned out to be the most promising lead compound for development of new bisubstrate inhibitors with better WC.

Table 5. Dissociation constants (K_D), and IWC of H89, staurosporine, BIM VIII, SGI-1776, and GSK690693

Compounds	K_D, nM (SE)		*IWC*†
	PKAcβ	S54L-PKAcβ	
H89	1.0 (0.1)	14.5 (0.6)	0.07
Staurosporine	0.71 (0.03)	0.61 (0.06)	1.2
BIM VIII	2,384 (27)	> 73,680	< 0.03
SGI-1776	1,163 (80)	1,698 (137)	0.7
GSK690693	61.5 (5.6)	82.5 (4.7)	0.8

† – IWC = K_D(PKAcβ)/K_D(S54L-PKAcβ). Measurements were performed in triplicate and the data variance was characterized with SE.

A study on L205R-PKAcα mutant revealed that PKI_{5-24} was 338-fold mutant-sparing [120]. The hydrophobic P + 1 pocket of PKAcα strongly interacts with Ile22 of PKI_{5-24}. Similarly, more hydrophobic GRL of S54L-PKAcβ fosters interactions (IWC values from 0.7 to 5.7) with compounds **3**, **4**, **11**, **12**, and **13**, all possessing a chiral spacer with a hydrophobic side chain. Furthermore, the S54L mutation in PKAcβ renders the mutated kinase non-targetable at Leu54 by irreversible inhibitor with the aim [69] of increasing the selectivity. Commercially available synthetic inhibitors usually possess mutant-sparing capability instead of WC. Their chemical structures have been optimized for inhibition of native proteins. Therefore, a mutation in the ligand-binding region usually leads to drug resistance. Thus, up to now the development of wild-type – sparing inhibitors for inhibition of mutated proteins is a challenging task. In this study, we could develop an inhibitor possessing the highest IWC value of 5.7.

5.3. Inhibitors and probes for PIM kinases (Paper III)

The expression level of PIM kinases is elevated in plasma cell malignancy [4]. Thus, recent success in development of PIM-selective inhibitors with low picomolar inhibitory potency [42] has intensified clinical testing of these inhibitors for the treatment of hematological cancers. ARC-inhibitors confer more selectivity to PKs thanks to the bisubstrate approach exploited to develop them [72]. Lately, we had developed pan-PIM-selective ARC-inhibitors [67] and now we went on with improving them.

5.3.1. Co-crystal structures ARC-1411 and ARC-3126 with PIM-1

Considering the impact that structural information may provide to the drug discovery iterative process, we attempted to obtain the first co-crystal structure of PIM with ARC-inhibitors. Here, we present the structures of ARC-1411 and ARC-3126 with PIM-1. ARC-1411 and ARC-3126 (**Paper III**, Figure 1) are structurally different in their adenosine analog moiety {4-(piperazin-1-yl)-7H-pyrrolo[2,3-d]pyrimidine *vs* 8-bromo-2-(methylene)benzo[4,5]thieno[3,2-d]pyrimidin-4-one, respectively} and the tether between the latter moiety and the peptide mimetic moiety (α,ω-nonanedioic acid *vs* 6-aminohexanoic acid, respectively). The PIM-1/ARC co-crystal structures were determined to 1.9-Å resolution (**Paper III**, Table S1). Their coordinates were deposited in the PDB (PDB 7OOV for ARC-1411 and PDB 7OOX for ARC-3126). All these structures feature one protein molecule in the asymmetric unit.

Importantly, these structures confirm the bisubstrate character of ARC inhibitors for PIM kinases [121], where the adenosine analog and peptide mimetic moieties bind to the ATP-pocket and substrate-protein pocket, respectively (Figure 5). Considering the structural similarity among PIM kinases, ARCs are also bisubstrate inhibitors to PIM-2 and PIM-3 (**Paper III**, Table 2) and the new co-crystal structures with PIM-1 can be used as models for PIM-2 and PIM-3. In the co-crystal structures of PIM-1 with ARC-1411 and ARC-3126, the adenosine analog moiety of the inhibitors is positioned in the ATP-binding site of PIM-1 and the peptide mimetic moiety binds on the protein substrate pocket. The peptide mimetic moiety of ARC-1411 is fully resolved in complex with PIM-1 compared to the complex with PKAcα [76]. ARC-1411 forms the traditional hydrogen bond between the nitrogen atom of pyrrole and the backbone of Glu121 of the PK hinge (Figure 5A). This positioning is similar to that of AMP-PNP in the crystal with PIM-1 [98]. Contrarily to it, ARC-1411 interacts with Ser46 of GRL by its first D-Arg residue (D-Arg1) (Figure 5A).

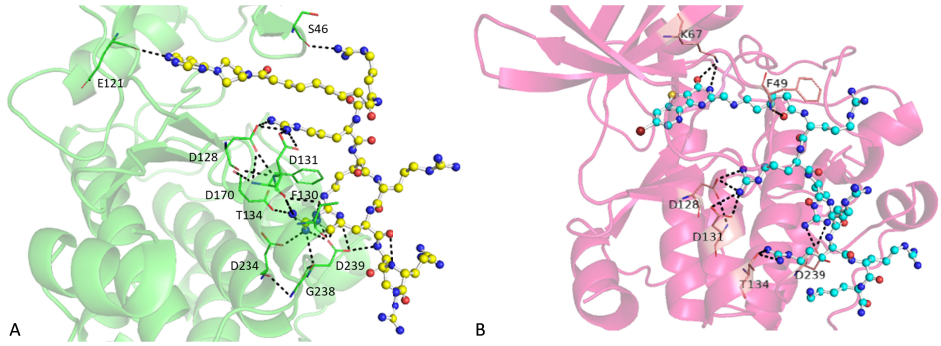

Figure 5. Interactions between ARCs and PIM-1. (A) Co-crystal structure of ARC-1411 with PIM-1; the kinase domain is depicted as a green cartoon and the inhibitor is shown in ball-and-stick representation (C atoms yellow, O atoms red, N atoms blue). (B) Co-crystal structure of ARC-3126 with PIM-1; PK is depicted as a pink cartoon and the inhibitor is shown in ball-and-stick representation (C atoms green, O atoms red, N atoms blue, S atom yellow, Br atom dark red). In (A) and (B), the AA residues of PIM-1 interacting with inhibitor are shown as sticks and are numbered; the hydrogen bonds are shown as dotted black lines.

Adenosine analog moiety of ARC-3126 (BPTP) does not mimic binding of AMP-PNP. The latter compound forms a hydrogen bond with the PK hinge. ARC-3126 rather anchors in the opposite side of this pocket and participates in a hydrogen bond network formed by the conserved Lys67 residue (Figure 5B). The non-traditional-hinge binding mode of BPTP in ARC-3126/PIM-1, similar to that of pyrimidinones and pyridazines in complex with PIM-1 [122], [123], is a distinctive element for its selectivity. ARC inhibitors with pyrimidinone derivatives as adenosine analog moiety are more selective to PIM kinases than to other basophilic PKs [121]. Contrarily, ARC-1411 inhibits a wide panel of basophilic PKs [76].

The peptide substrate pocket of the PIM-1 is also involved in interactions with ARC-1411 and ARC-3126. The peptide mimetic moieties of these two ARC-inhibitors make the same interactions with PIM-1 (Figure 5). D-Arg2 in the structure of the ARC-inhibitors interacts with Asp128 and Asp131 of PIM-1, D-Arg3 with Asp239 of PIM-1, D-Arg5 with Phe130, Asp170, and Thr134 of PIM-1 (Figure 5). D-Arg4 and D-Arg6 do not make interactions with the protein. Additionally, D-Arg5 of ARC-1411 makes additional interactions with Asp234 and Gly238. PIM-1 has been shown to have a strong preference for substrates with basic residues, particularly Arg, at positions −5 and −3 from the phosphorylation site [123]. The Arg residues at these two positions in the consensus peptide substrate of PIM Pimtide interact with the same PIM-1 residues as ARC-1411 and ARC-3126 do. Thus, these inhibitors have the capacity of blocking protein-protein interaction involving PIM kinases and their protein substrates, similarly to a structurally different inhibitor that also reveals multiple interactions with residues of the substrate-binding site [124].

5.3.2. Design of new inhibitors and their characterization

A new set of ARC-compounds was designed proceeding from the lead compound ARC-3126 ($K_{D,PIM-1}$ = 1.8 nM; **Paper III**, Figure 1), because of the higher selectivity of its adenosine analog moiety compared to that of ARC-1411. This affinity value was determined in a binding/displacement assay using ARC-1451 ($K_{D,PIM-1}$ = 2 nM) as the photoluminescent probe (**Paper III**, Figure S2). From the crystal structure data, knowing that D-Arg1, D-Arg4,and D-Arg6 of ARC-3126 do not make major contacts with PIM-1, these residues were removed from the new ARC inhibitors to reduce their complexity and decrease their binding to nucleic acids [125] in cells. Potentially, these new structures were expected to demonstrate less non-specific binding to components of biochemical assays due to a fewer number of D-Arg residues in them. Besides, D-Arg4 was replaced by Gly residue to conserve the positioning of D-Arg5. The C-terminal D-Lys was retained for potential labeling of inhibitors at this AA. A longer linker (8-aminooctanoic acid, Aoc) than that in ARC-3126 (6-aminohexanoic acid) was used to account for the approximate dimension of D-Arg1 in ARC-3126 and conserve the optimal positioning of the remaining residues (Table 6). Different types of the linker were also tested (Table 6).

Compound **14** (possessing a smaller number of D-Arg residues and Aoc linker) revealed a K_D value of 11.4 nM compared to K_D value of 1.8 nM for ARC-3126. The modifications performed on ARC-3126 did not change much its affinity toward PIM-1 (Table 6). Besides, PKAcα, another basophilic PK binding to Arg-rich ARCs with high-affinity [72], was used in binding/displacement assay for comparison of selectivity of compounds toward PIM-1. Compound **14** was over 50-fold less selective toward PIM-1 than ARC-3126. Next, the adenosine analog moiety BPTP in compound **14** was replaced in compound **15** by BBTP, reported to have high affinity and selectivity to PIM kinases [122]. In doing so, the selectivity was increased 9.3-fold from compound **14** to compound **15**. The latter compound had a K_D value of 0.4 nM to PIM-1 (Table 6). Moreover, compounds **14** and **15** are structurally simpler than ARC-3126. From the synthesis point of view, they are easier to obtain than ARC-3126.

ARC-3126 and compounds **14** and **15** were assessed in an inhibition panel of PKs. They were strongly inhibiting PIM kinases (**Paper III**, Section 2.4).

Table 6. Structures of tested ARC-inhibitors and their affinities toward PIM kinases and PKAcα

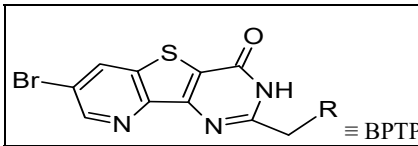

≡ BPTP

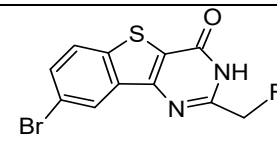

≡ BBTP

Compound #	Structure	K_D, nM (PIM-1)[a]	K_D, nM (PIM-2)[a]	K_D, nM (PIM-3)[a]	K_D, nM (PKAcα)[a]
ARC-3126	BPTP-Ahx-(D-Arg)$_6$-D-Lys-NH_2	1.8 (0.7)	2.9 (0.5)	2.0 (0.5)	> 18,460
14	BPTP-**Aoc-(D-Arg)$_2$-Gly-D-Arg**-D-Lys-NH_2	11.4 (1)	64 (8)	5.2 (1)	2,250 (411)
15	**BBTP**-Aoc-(D-Arg)$_2$-Gly-D-Arg-D-Lys-NH_2	0.4 (0.1)	3.8 (0.2)	2.0 (0.4)	853 (28)
16	BBTP-**Amt**-(D-Arg)$_2$-Gly-D-Arg-D-Lys-NH_2	0.7 (0.2)	9.9 (0.8)	7 (1)	1,502 (266)
17	BBTP-**Tap**-(D-Arg)$_2$-Gly-D-Arg-D-Lys-NH_2	1.8 (0.3)	20 (4)	6.6 (1.4)	> 18,210
18	BBTP-**Hyp-Aoc**-(D-Arg)$_2$-Gly-D-Arg-D-Lys-NH_2	37.8 (9)	447.4 (52)	30.4 (6.5)	> 20,590
AZD1208	Not shown	5.3 (1)	11.8 (2)	2.3 (0.4)	> 83,000
PIM peptide	(D-Arg)$_2$-Gly-D-Arg-D-Lys-NH_2	> 11,490	> 46,020	> 16,420	> 89,000

BPTP – 7-bromo-2-(methylene)pyrido[4,5]thieno[3,2-d]pyrimidin-4-one moiety; Ahx – 6-aminohexanoic acid moiety; Aoc – 8-aminooctanoic acid moiety; BBTP – 8-bromo-2-(methylene)[1]benzothieno[3,2-d]pyrimidin-4-one moiety; Amt – [4-(aminomethyl)-1H-1,2,3-triazol-1-yl]acetic acid moiety; Tap – 5-(1H-1,2,3-triazol-4-yl)pentanoic acid moiety; Hyp – hydroxyproline. [a] K_D values were determined in binding/displacement assays with TGLI or FA readout using probes ARC-1451, ARC-1188, or ARC-583 [77], [100]. The full structures of ARCs are depicted in **Paper III**, Table S2. Mean values ± SEM are shown (N = 2).

PKAcα prefers flexible linkers between the adenosine analog and peptide mimetic moieties of ARCs [76]. The linker Aoc in compounds **14** and **15** is highly flexible. Rigidified linkers comprising 1,2,3-triazole were tested as alternatives to Aoc. Besides, 1,2,3-triazole moieties are attractive tethers because they are stable to cellular degradation and capable of hydrogen bonding which can improve the inhibitor's solubility. The compatibility of click chemistry with solid-phase peptide synthesis [126] was confirmed for ARC inhibitors by producing compounds **16** and **17** incorporating 1,2,3-triazozle linkers (**Paper III**, Supplementary methods). [4-(aminomethyl)-1H-1,2,3-triazol-1-yl]acetic acid (Amt) was used in **16** as the linker. The affinity and selectivity of **16** are comparable to those of compound **15** (Table 6). Their comparability suggests that Aoc and Amt can be interchangeable. The use of another linker, 5-(1H-1,2,3-triazol-4-yl)pentanoic acid (Tap) yielded compound **17**, which has over

5.5-fold higher selectivity compared to **16**. It has a K_D value of 1.8 nM toward PIM-1 (Table 6). It has been shown that ARC-inhibitors with hydroxyproline (Hyp)-incorporating linkers have better selectivity to PIM kinases [121]. Thereby, **15** was modified by insertion of Hyp between BBTP and Aoc. It resulted in compound **18** with over 3.5-fold worse selectivity toward PIM-1 compared to **15**, suggesting a worse positioning of the peptide mimetic moiety of **18** if in complex with PIM-1.

The binding of the distinct peptide mimetic moiety of compounds **14**-**18** (PIM peptide) to PIM-1 was also tested. It revealed only weak affinity, possessing a K_D value of over 10 μM (Table 6).

Finally, the tested compounds revealed almost the same affinity and selectivity to PIM-3 compared to PIM-1 while they demonstrated lower affinity to PIM-2 (except for ARC-3126 which showed similar affinity toward all PIM kinases; Table 6). Compounds **15** and **17** were labeled with the fluorescent dye Cyanine 5 (Cy5) and 5-TAMRA, resulting in fluorescent probes that were capable of crossing the cell plasma membrane (**Paper III**, Section 2.6). Besides, **15** was colocalized with fluorescent-protein-tagged PIM-1 (**Paper III**, Figure 7). The fluorescence background signal from adsorption of fluorescent probes to plastic was lower with Cy5-labeled ARCs, compared to 5-TAMRA-labeled probes. If compounds **15** and **17** were labeled with sulfonated Cy5 dye, the resulting compounds were not capable of penetrating the cell plasma membrane.

5.4. Development of assays for PKAcα and PIM-2 (Papers I, III, and unpublished data)

5.4.1. The AbARC assay

Although the activity level of extracellular PKAcα in the blood serum of cancer patients is increased by 5-fold compared to healthy people [19], the concentration of PKAcα in serum samples is still very low and thus not detectable with routine liquid chromatography/tandem mass spectrometry analysis [127] and most of screening assays. Therefore, new sensitive and specific analytical assays are needed to assess its expression level and activity in bodily fluids, tissue extracts, cell lysates, and cells. So, the AbARC assay was developed for this purpose.

The AbARC assay was constructed utilizing the competitiveness of the PKAcα isoform-specific inhibitory antibody with ARC-Lum(Fluo) probes (Figure 6). The assay is based on specific capture of PKAcα to mAb(D38C6)-immobilized immunoaffinity surface and consecutive elution of the bound active enzyme from the surface using the high-affinity ARC-Lum(Fluo) probe ARC-1063 (Scheme 3; K_D value of 10 pM toward PKAcα [100]). The latter probe was concomitantly used as the detection reagent. It was possible to retrieve PKAcα from the surface with the eluent and nothing eluted from the surface when it was not functionalized, suggesting that there was no capture of

PKAcα on the surface (Figure 7). In immobilizing mAb(D38C6)-BTN on the surface first and thereafter capturing the analyte PKAcα (direct immunocapture mode), we had noticed that the efficiency of capture was low. To determine PKAcα in complicated solutions, the assay had to be more sensitive. Then, we tested the immobilization of mAb(D38C6)-BTN and capture of PKAcα in a single step concomitantly (indirect immunocapture mode). It resulted in higher immunocapture efficiency of PKAcα on the surface (**Paper I**, Table 1). Besides, the indirect capture mode also reduced the assay time.

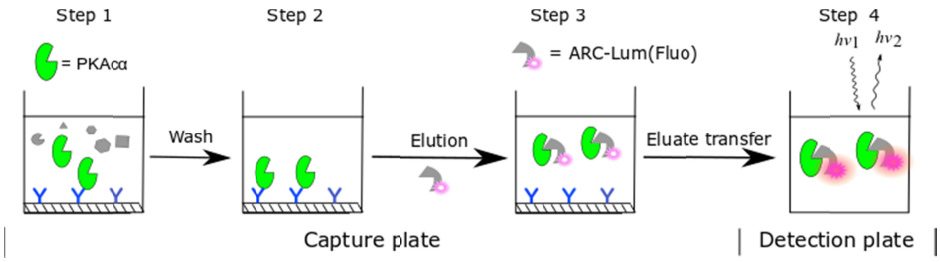

Figure 6. Scheme of the AbARC assay. PKAcα is bound to mAb(D38C6)-BTN functionalized surface (step 1), the capture microtiter well is washed (step 2), the solution of the photoluminescent ARC-probe is added that displaces PKAcα from the surface complex (step 3); thereafter the eluate is transferred to the low-binding surface detection microtiter plate and the intensity of TGLI signal is measured (step 4).

A

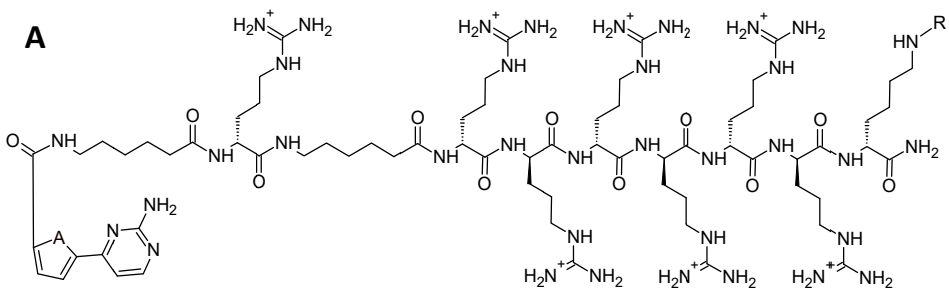

B

Code	A	R
ARC-1063	S	Alexa Fluor 647
ARC-1139	Se	PromoFluor-647

Scheme 3. Structures and codes of ARC-Lum(Fluo) probes. (A) Structure of ARC-1063 and ARC-1139, (B) Table with ARC codes.

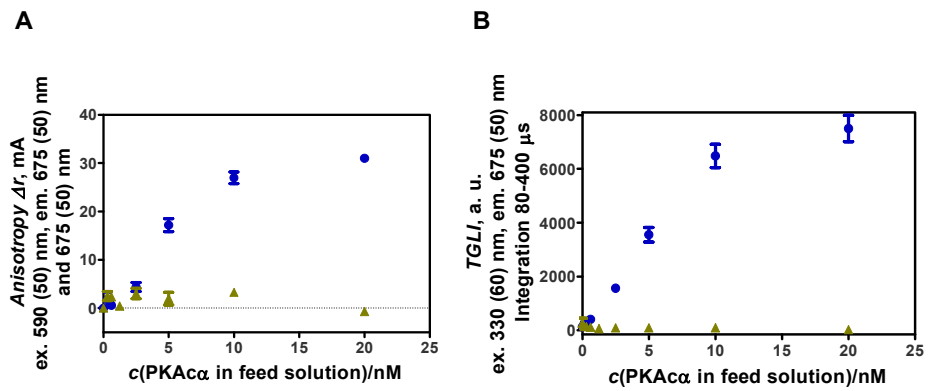

Figure 7. AbARC assay window in protocol "A" (**Paper I**, Section 2.4). (A) FA readout and (B) TGLI readout without (green ▲) and with (blue ●) immobilization of mAb(D38C6)-BTN (6 pmol) onto the streptavidin surface. ARC-1063 (0.09 pmol, 2 nM) was used as eluent and detection reagent. Measurements were performed in triplicate and variance was characterized with SEM.

Parameters of association/dissociation kinetics should be considered in constructing an end-point binding assay. Dissociation rate of the mAb(D38C6)/PKAcα complex determines how long it takes to reach equilibrium. To be applicable for measurements with reasonable waiting time, the processes should occur quickly [128]. Short half-lives of elution (2 min; **Paper I**, Figure S10) enabled the development of the fast AbARC assay. Furthermore, ARC-1139 used in the final version of AbARC assay incorporates a selenophene-comprising polycyclic aromatic fragment as the adenosine analog moiety. The selenophene-comprising moiety provides higher brightness to the probe, compared with the thiophene-comprising counterpart [79]. Higher brightness is beneficial to achieve better sensitivity and lower the limit of quantification (LoQ) of the assay. In using the thiophene-comprising probe ARC-1063, the lowest amount of PKAcα that could be quantified was 59 fmol. On the other hand, in using its selenophene-comprising counterpart ARC-1139, PKAcα could be quantified at 25 times lower level (2.3 fmol; **Paper I**, Figure 5). The sensitivity of AbARC assay can be increased in immobilizing mAb(D38C6)-BTN on microscopic beads [93].

AbARC assay keeps the enzyme active thanks to a gentle elution at physiological pH unlike in most immunoprecipitation protocols where the elution is performed under acidic conditions. Besides, a solution with low pH value was used in inhibition assay to degrade PKAcα and stop catalysis (**Paper I**, Section 2.3). The elution in final version of AbARC assay is performed for 10 min in reaching the maximal signal (**Paper I**, Figure S10), while 30 min were necessary for reaching only half maximal signal in an alternative assay [129]. Three elutions were needed for achieving elution efficiency of 78% in the

AbARC assay. These short 10-min cycles permitted the development of the timesaving AbARC assay. Differently from ELISA assays, the application of a second, orthogonal antibody is not required in the AbARC assay. Instead, a PK group-selective photoluminescent probe is used for analysis of PKAcα. ARC-probes are synthetic organic compounds, and they have the advantage of being proteolytically more stable than antibodies.

Furthermore, the cellular concentrations of PKAcα in cells determined with the AbARC assay (**Paper I**, Figure 6) are close to the PKAcα concentration of 200 nM in HEK293T cells determined with other methods previously [130]. The developed AbARC assay allows specifically determining PKAcα in lysates where one molecule of PKAcα is found among 1 200 (HeLa), 17 000 (SKOV-3), 15 000 (St-T1b), and 12 000 (HCC-44) other protein molecules. Given an average MW of eukaryotic cell protein of 50 kDa (BNID 108030; www.bionumbers.hms.harvard.edu), these values were obtained from the ratio of total protein molar concentration in the lysate determined by Bradford assay over PKAcα molar concentration in the lysate determined by AbARC assay (**Paper I**, Figure S9A and S9B). The AbARC assay is economical from the point of view of both labor input and use of chemicals. Furthermore, only 35 µg of mAb(D38C6)-BTN are needed to analyze 384 samples with the AbARC assay. In addition, monoclonal overlapping epitope-competitive antibodies against other AGC kinases could be produced at low cost by genetic engineering by periplasmic expression of recombinant Fab fragments [61] in low cost *E.* coli expression system [131]. It will permit the adaptation of the AbARC assay to other AGC kinases.

5.4.2. Surface sandwich assay for the measurement of PIM-2 concentration (AbARC-2 assay)

PIM-2 is largely expressed in both leukemia and solid tumors. It plays an important role in promoting cell survival and preventing apoptosis [133]. Therefore, new analytical sensitive and specific methods are needed to assess its expression level and activity in cells, cell lysates, and tissue extracts. To our knowledge, there are few reports on protein analysis assays based on formation of a three-component complex [134] on solid surface that use the combination of a small-molecule inhibitor and specific antibody as capture/detection reagents [135].

To establish a sandwich ELISA-adapted assay, we have substituted an ARC-inhibitor-based capture molecule for the capture antibody. ARC-inhibitors are synthetic mid-sized organic molecules which feature several advantages as compared to an antibody, such as shorter generation time, lower costs of manufacturing, the lack of batch-to-batch variability, higher modifiability, and better thermal stability. Another distinctive feature of the ARC-utilizing assay that might be physiologically relevant is that only the active kinase is captured, whereas the non-active (*e.g.*, denatured) PIM-2 is washed out during the process.

For the surface AbARC-2 assay, ARC-2073, a biotinylated derivative of compound **15** was synthesized (**Paper III**, Table S2). Following immobilization of ARC-2073 onto a streptavidin surface, PIM-2 was captured from a solution containing the recombinant protein. Thereafter, the captured PIM-2 was detected using rabbit anti-PIM-2 antibody D1D2 and visualized with a europium chelate-labeled secondary goat antibody against rabbit IgG (G0506) (scheme of AbARC-2 assay; **Paper III**, Figure 4A). The emission spectrum of G0506 presents several major peaks at 596 nm, 616 nm, and 694 nm (Figure 8A), with the peak at 616 nm being the highest (main) peak. We had tested three commercial filters with two different bandpass widths [590 (50) nm, 615 (10) nm, and 675 (50) nm] in PHERAstar microplate reader, so to cover these peaks. We assessed the sensitivity of the AbARC-2 assay at these peaks (Figure 8B-C). The sensitivity is the best (slope of curve 6200 a. u. nM^{-1}) in using the filter [590 (50) nm] since it covers a part of the main emission peak. Besides, non-specific binding of catcher ARC-2073 is negligible here. With no analyte PIM-2, there is no signal irrespective of the peak at which the signal is acquired.

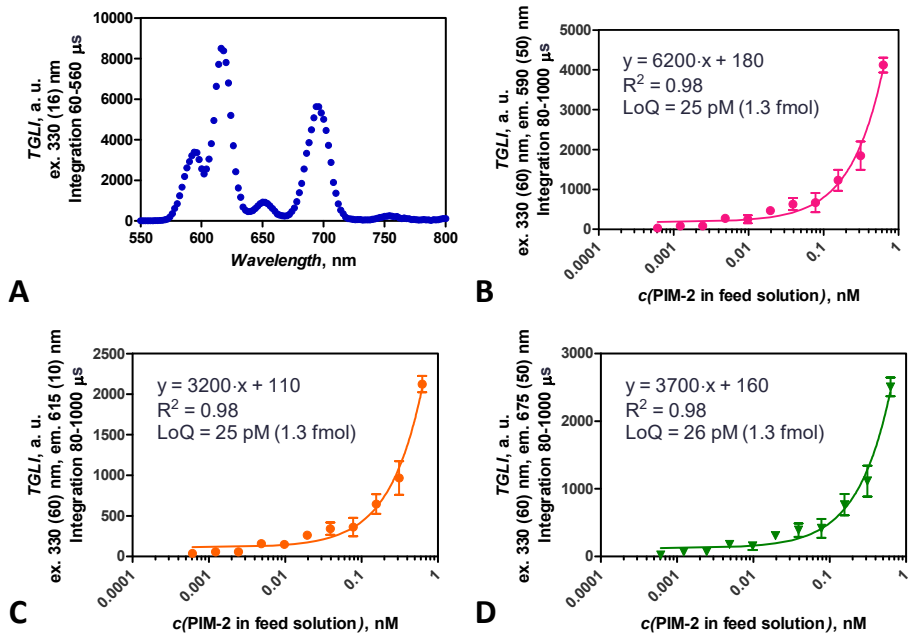

Figure 8. Europium chelate emission spectrum and calibration curve of the AbARC-2 assay for measurement of concentration of PIM-2. (A) Time-resolved emission spectrum of the europium chelate-labeled secondary goat antibody against rabbit IgG in solution. Calibration curve for PIM-2 analysis [immobilized ARC-2073 (4 pmol), detection with D1D2 (84 fmol) and G0506 (110 fmol)] obtained with filters 590 (50) nm (B), 615 (10) nm (C), and 675 (50) nm (D). Measurements were performed in triplicate and variance was characterized with SEM.

With disregard for the filter used, the lowest quantifiable concentration of PIM-2 was 25 ± 1 pM (quantification range from 25 pM to 625 pM), pointing to high sensitivity of the AbARC-2 assay affording the measurement (LoQ) of 1.3 fmol (44 pg) of PIM-2 in the sample (50 μL). This sensitivity is thus advantageous *versus* the PIM-2 ELISA kit from ELK Biotechnology (product #ELK6492) which has quantification limit of 1.8 fmol.

To assess the selectivity of the AbARC-2 assay, ARC-2073-coated surface was treated with solutions of PIM-1, PIM-3, and DYRK1α (an off-target PK of ARC-2073). These kinases were not detected with the pair of detection reagents D1D2/G0506 (**Paper III**, Figure S2) confirming that D1D2 is specifically binding to PIM-2. In essence, the developed assay can be used for screening antibodies orthogonal to ARC-2073. On the other hand, the developed method can be potentially adapted for quantitative detection of PIM-1 or PIM-3 by switching to the appropriate primary antibodies. According to the literature, D1D2 was used for the specific detection of PIM-2 in cell lysates [136]. Unfortunately, the AbARC-2 assay did not work reliably in complex biological solutions such as crude cell lysates (**Paper III**, Figure S3) unlike the original AbARC assay, probably due to matrix effects (presence of other biological molecules) on the stability of ARC-2073/PIM-2 complex in such solutions. We have worked on reversing the AbARC-2 assay format to capture PIM-2 with a surface-immobilized antibody to overcome this issue. A reliable calibration curve was not obtained in that format. It may be due to hindrance of binding of europium chelate-labeled ARC when D1D2 is already bound to PIM-2. This issue could be overcome in using a different PIM-2 antibody.

6. CONCLUSIONS

The current thesis is focused on the design, synthesis, characterization, and application of bifunctional inhibitors of PKs, conjugates of an adenosine analogue heteroaromatic moiety and substrate peptide mimetic D-Arg-rich fragment, covalently tethered by a linker (ARCs). The literature overview briefly introduces the basics of PKs, antibodies, photoluminescence, inhibitors of PKs, and methods involved in PK studies. These topics are relevant regarding the main results of this thesis, which are summarized as follows:

- Inhibitory properties of the monoclonal antibody mAb(D38C6) were discovered upon screening antibodies against PK PKAcα if using binding-responsive photoluminescent ARC-Lum(Fluo) probes. The rationale for employing such inhibitory antibodies in pathologies' treatment was discussed.
- Epitope restructuring caused by binding of mAb(D38C6) to PKAcα led to dissociation of ARC-Lum(Fluo) probe from the complex with the kinase. The discovered phenomenon was used to work-out AbARC assay for the analysis of PKAcα in cell lysates.
- TGLI decay of ARC-1085 and ARC-1086 in complexes with wild-type (wt) PKAcβ or its mutated form S54L-PKAcβ shed light on the flexibility of these two kinase molecules. FA- and TGLI-based binding/displacement assays were developed for screening inhibitors of new protein targets, wt PKAcβ and its mutated form S54L-PKAcβ.
- The effect of different structural elements of inhibitors on PKAcβ/S54L-PKAcβ selectivity was studied. The use of a hydrophobic chiral spacer in ARC led to a wild-type-sparing inhibitor, compound **11**, possessing high affinity (K_D of 5.0 nM for S54L-PKAcβ) and considerable selectivity (IWC of 5.7) over the PKAcβ. Structure of compound 11 can further modified to increase its IWC. Staurosporine can serve as lead compound for constructing of new wild-type-sparing inhibitors.
- X-ray analysis of PIM-1/ARC co-crystals confirmed the bisubstrate binding mode of ARCs to PIM kinases. Guided by crystal structures, structurally simplified ARC inhibitors and ARC-based fluorescent probes were constructed. New ARC-probes were efficiently taken up by cultured cells. Co-localization of the probes with fluorescent protein-fused PIM-1 was shown in confocal microscopy experiments in living cells.
- The AbARC-2 assay was developed for the analysis of PIM-2 protein in biological solutions with proceeding from the new knowledge about formation of the three-component complex ARC-2073/PIM-2/mAb(D1D2) on solid support.

REFERENCES

[1] P. Cohen, “Protein kinases – the major drug targets of the twenty-first century?,” *Nat Rev Drug Discov*, vol. 1, no. 4, pp. 309–315, Apr. 2002, doi: 10.1038/nrd773.

[2] C. Gil *et al.*, “COVID-19: Drug Targets and Potential Treatments,” *J. Med. Chem.*, p. acs.jmedchem.0c00606, Jun. 2020, doi: 10.1021/acs.jmedchem.0c00606.

[3] R. Roskoski, “A historical overview of protein kinases and their targeted small molecule inhibitors,” *Pharmacological Research*, vol. 100, pp. 1–23, Oct. 2015, doi: 10.1016/j.phrs.2015.07.010.

[4] N. A. Keane, M. Reidy, A. Natoni, M. S. Raab, and M. O’Dwyer, “Targeting the Pim kinases in multiple myeloma,” *Blood Cancer Journal*, vol. 5, no. 7, pp. e325–e325, Jul. 2015, doi: 10.1038/bcj.2015.46.

[5] A. C. Anderson, “The Process of Structure-Based Drug Design,” *Chemistry & Biology*, vol. 10, no. 9, pp. 787–797, Sep. 2003, doi: 10.1016/j.chembiol.2003.09.002.

[6] S. S. Taylor, E. Radzio-Andzelm, Madhusudan, X. Cheng, L. Ten Eyck, and N. Narayana, “Catalytic Subunit of Cyclic AMP-Dependent Protein Kinase,” *Pharmacology & Therapeutics*, vol. 82, no. 2–3, pp. 133–141, May 1999, doi: 10.1016/S0163-7258(99)00007-8.

[7] S. Lemeer and A. J. R. Heck, “The phosphoproteomics data explosion,” *Curr Opin Chem Biol*, vol. 13, no. 4, pp. 414–420, Oct. 2009, doi: 10.1016/j.cbpa.2009.06.022.

[8] G. Manning, D. B. Whyte, R. Martinez, T. Hunter, and S. Sudarsanam, “The protein kinase complement of the human genome,” *Science*, vol. 298, p. 1912, 2002.

[9] P. A. Schwartz and B. W. Murray, “Protein kinase biochemistry and drug discovery,” *Bioorganic Chemistry*, vol. 39, no. 5–6, pp. 192–210, Dec. 2011, doi: 10.1016/j.bioorg.2011.07.004.

[10] N. C. Price and L. Stevens, *Fundamentals of enzymology: the cell and molecular biology of catalytic proteins*, 3rd ed. Oxford ; New York: Oxford University Press, 1999.

[11] L. R. Pearce, D. Komander, and D. R. Alessi, “The nuts and bolts of AGC protein kinases,” *Nat. Rev. Mol. Cell Biol.*, vol. 11, p. 9, 2010.

[12] D. A. Walsh, D. B. Glass, and R. D. Mitchell, “Substrate diversity of the cAMP-dependent protein kinase: regulation based upon multiple binding interactions,” *Curr. Opin. Cell Biol.*, vol. 4, no. 2, pp. 241–251, Apr. 1992, doi: 10.1016/0955-0674(92)90039-f.

[13] P. Zhang *et al.*, “Single Turnover Autophosphorylation Cycle of the PKA RIIβ Holoenzyme,” *PLoS Biol.*, vol. 13, p. e1002192, 2015.

[14] B. S. Skålhegg and K. Taskén, “Specificity in the cAMP/PKA signaling pathway. differential expression, regulation, and subcellular localization of subunits of PKA,” *Front. Biosci.*, vol. 2, pp. d331-342, Jul. 1997, doi: 10.2741/a195.

[15] C. Walker *et al.*, “Cushing’s syndrome driver mutation disrupts protein kinase A allosteric network, altering both regulation and substrate specificity,” *Sci. Adv.*, vol. 5, no. 8, p. eaaw9298, Aug. 2019, doi: 10.1126/sciadv.aaw9298.

[16] S. Espiard *et al.*, “Activating PRKACB somatic mutation in cortisol-producing adenomas,” *JCI Insight*, vol. 3, no. 8, Apr. 2018, doi: 10.1172/jci.insight.98296.

[17] M. J. Knape *et al.*, “Molecular Basis for Ser/Thr Specificity in PKA Signaling,” *Cells*, vol. 9, no. 6, p. 1548, Jun. 2020, doi: 10.3390/cells9061548.
[18] D. H. Bhang *et al.*, “Characteristics of extracellular cyclic AMP-dependent protein kinase as a biomarker of cancer in dogs,” *Vet Comp Oncol*, vol. 15, no. 4, pp. 1585–1589, Dec. 2017, doi: 10.1111/vco.12304.
[19] Y. S. Cho, Y. N. Lee, and Y. S. Cho-Chung, “Biochemical characterization of extracellular cAMP-dependent protein kinase as a tumor marker,” *Biochem Biophys Res Commun*, vol. 278, no. 3, pp. 679–684, Nov. 2000, doi: 10.1006/bbrc.2000.3853.
[20] M. M. Vetter, H.-M. Zenn, E. Méndez, H. van den Boom, F. W. Herberg, and B. S. Skålhegg, “The testis-specific Cα2 subunit of PKA is kinetically indistinguishable from the common Cα1 subunit of PKA,” *BMC Biochem*, vol. 12, no. 1, p. 40, 2011, doi: 10.1186/1471-2091-12-40.
[21] D. A. Johnson, P. Akamine, E. Radzio-Andzelm, M. Madhusudan, and S. S. Taylor, “Dynamics of cAMP-dependent protein kinase,” *Chem. Rev.*, vol. 101, p. 2243, 2001.
[22] A. Kvissel, “Induction of Cβ splice variants and formation of novel forms of protein kinase A type II holoenzymes during retinoic acid-induced differentiation of human NT2 cells,” *Cellular Signalling*, vol. 16, no. 5, pp. 577–587, May 2004, doi: 10.1016/j.cellsig.2003.08.014.
[23] S. S. Taylor *et al.*, “PKA Cβ: a forgotten catalytic subunit of cAMP-dependent protein kinase opens new windows for PKA signaling and disease pathologies,” *Biochemical Journal*, vol. 478, no. 11, pp. 2101–2119, Jun. 2021, doi: 10.1042/BCJ20200867.
[24] A. Kreegipuu, N. Blom, S. Brunak, and J. Järv, “Statistical analysis of protein kinase specificity determinants,” *FEBS Lett.*, vol. 430, no. 1–2, pp. 45–50, Jun. 1998, doi: 10.1016/s0014-5793(98)00503-1.
[25] D. M. Thomson *et al.*, “AMP-activated protein kinase phosphorylates transcription factors of the CREB family,” *Journal of Applied Physiology*, vol. 104, no. 2, pp. 429–438, Feb. 2008, doi: 10.1152/japplphysiol.00900.2007.
[26] B.-R. Yan *et al.*, “PKACs attenuate innate antiviral response by phosphorylating VISA and priming it for MARCH5-mediated degradation,” *PLoS Pathog*, vol. 13, no. 9, p. e1006648, Sep. 2017, doi: 10.1371/journal.ppat.1006648.
[27] G. G. Jinesh, S. Mokkapati, K. Zhu, and E. E. Morales, “Pim kinase isoforms: devils defending cancer cells from therapeutic and immune attacks,” *Apoptosis*, vol. 21, no. 11, pp. 1203–1213, Nov. 2016, doi: 10.1007/s10495-016-1289-3.
[28] Y. Alvarado, F. J. Giles, and R. T. Swords, “The PIM kinases in hematological cancers,” *Expert Review of Hematology*, vol. 5, no. 1, pp. 81–96, Feb. 2012, doi: 10.1586/ehm.11.69.
[29] O. Kim, T. Jiang, Y. Xie, Z. Guo, H. Chen, and Y. Qiu, “Synergism of cytoplasmic kinases in IL6-induced ligand-independent activation of androgen receptor in prostate cancer cells,” *Oncogene*, vol. 23, no. 10, pp. 1838–1844, Mar. 2004, doi: 10.1038/sj.onc.1207304.
[30] P. V. Hornbeck, B. Zhang, B. Murray, J. M. Kornhauser, V. Latham, and E. Skrzypek, “PhosphoSitePlus, 2014: mutations, PTMs and recalibrations,” *Nucleic Acids Res*, vol. 43, no. Database issue, pp. D512-520, Jan. 2015, doi: 10.1093/nar/gku1267.
[31] A. Macdonald, D. G. Campbell, R. Toth, H. McLauchlan, C. J. Hastie, and J. S. C. Arthur, “Pim kinases phosphorylate multiple sites on Bad and promote 14-3-3

binding and dissociation from Bcl-XL," *BMC Cell Biol*, vol. 7, p. 1, Jan. 2006, doi: 10.1186/1471-2121-7-1.
[32] Y. Xie *et al.*, "The 44 kDa Pim-1 kinase directly interacts with tyrosine kinase Etk/BMX and protects human prostate cancer cells from apoptosis induced by chemotherapeutic drugs," *Oncogene*, vol. 25, no. 1, pp. 70–78, Jan. 2006, doi: 10.1038/sj.onc.1209058.
[33] G. Zhu *et al.*, "Exceptional Disfavor for Proline at the P+1 Position among AGC and CAMK Kinases Establishes Reciprocal Specificity between Them and the Proline-directed Kinases," *J. Biol. Chem.*, vol. 280, no. 11, pp. 10743–10748, Mar. 2005, doi: 10.1074/jbc.M413159200.
[34] A. N. Bullock, J. Debreczeni, A. L. Amos, S. Knapp, and B. E. Turk, "Structure and Substrate Specificity of the Pim-1 Kinase," *J. Biol. Chem.*, vol. 280, no. 50, pp. 41675–41682, Dec. 2005, doi: 10.1074/jbc.M510711200.
[35] T. B. Trinh, Q. Xiao, and D. Pei, "Profiling the Substrate Specificity of Protein Kinases by On-Bead Screening of Peptide Libraries," *Biochemistry*, vol. 52, no. 33, pp. 5645–5655, Aug. 2013, doi: 10.1021/bi4008947.
[36] M. A. Bogoyevitch, R. K. Barr, and A. J. Ketterman, "Peptide inhibitors of protein kinases—discovery, characterisation and use," *Biochimica et Biophysica Acta (BBA) - Proteins and Proteomics*, vol. 1754, no. 1–2, pp. 79–99, Dec. 2005, doi: 10.1016/j.bbapap.2005.07.025.
[37] K. S. Kalichamy *et al.*, "PIM-Related Kinases Selectively Regulate Olfactory Sensations in *Caenorhabditis elegans*," *eNeuro*, vol. 6, no. 4, p. ENEURO.0003-19.2019, Jul. 2019, doi: 10.1523/ENEURO.0003-19.2019.
[38] N. S. Magnuson, Z. Wang, G. Ding, and R. Reeves, "Why target PIM1 for cancer diagnosis and treatment?," *Future Oncology*, vol. 6, no. 9, pp. 1461–1478, Sep. 2010, doi: 10.2217/fon.10.106.
[39] N. An, A. S. Kraft, and Y. Kang, "Abnormal hematopoietic phenotypes in Pim kinase triple knockout mice," *J Hematol Oncol*, vol. 6, p. 12, Jan. 2013, doi: 10.1186/1756-8722-6-12.
[40] K. Miyakawa *et al.*, "PIM kinases facilitate lentiviral evasion from SAMHD1 restriction via Vpx phosphorylation," *Nat Commun*, vol. 10, no. 1, p. 1844, Dec. 2019, doi: 10.1038/s41467-019-09867-7.
[41] B. Zimmermann, J. A. Chiorini, Y. Ma, R. M. Kotin, and F. W. Herberg, "PrKX Is a Novel Catalytic Subunit of the cAMP-dependent Protein Kinase Regulated by the Regulatory Subunit Type I," *J. Biol. Chem.*, vol. 274, no. 9, pp. 5370–5378, Feb. 1999, doi: 10.1074/jbc.274.9.5370.
[42] P. D. Garcia *et al.*, "Pan-PIM kinase inhibition provides a novel therapy for treating hematologic cancers," *Clin. Cancer Res.*, vol. 20, no. 7, pp. 1834–1845, Apr. 2014, doi: 10.1158/1078-0432.CCR-13-2062.
[43] J. M. Cruse and R. E. Lewis, *Atlas of Immunology.* 2010. Accessed: Aug. 09, 2020. [Online]. Available: https://public.ebookcentral.proquest.com/choice/publicfullrecord.aspx?p=5311921
[44] C. Janeway, Ed., *Immunobiology: the immune system in health and disease*, 5. ed. New York, NY: Garland Publ. [u.a.], 2001.
[45] M. Khoshnejad *et al.*, "Development of Novel DNA-Encoded PCSK9 Monoclonal Antibodies as Lipid-Lowering Therapeutics," *Molecular Therapy*, vol. 27, no. 1, pp. 188–199, Jan. 2019, doi: 10.1016/j.ymthe.2018.10.016.

[46] E. M. S. Stennett, M. A. Ciuba, and M. Levitus, “Photophysical processes in single molecule organic fluorescent probes,” *Chem. Soc. Rev.*, vol. 43, no. 4, pp. 1057–1075, 2014, doi: 10.1039/C3CS60211G.
[47] J. R. Lakowicz, *Principles of fluorescence spectroscopy*, Third edition, Corrected at 4. printing. New York, NY: Springer, 2010.
[48] J. Kuijt, F. Ariese, U. A. Th. Brinkman, and C. Gooijer, “Room temperature phosphorescence in the liquid state as a tool in analytical chemistry,” *Analytica Chimica Acta*, vol. 488, no. 2, pp. 135–171, Jul. 2003, doi: 10.1016/S0003-2670(03)00675-5.
[49] I. Medintz and N. Hildebrandt, Eds., *FRET - Förster Resonance Energy Transfer: from theory to applications*. Weinheim: Wiley-VCH, 2013.
[50] H. Chen, H. L. Puhl, S. V. Koushik, S. S. Vogel, and S. R. Ikeda, “Measurement of FRET efficiency and ratio of donor to acceptor concentration in living cells,” *Biophys J*, vol. 91, no. 5, pp. L39-41, Sep. 2006, doi: 10.1529/biophysj.106.088773.
[51] A. K. Hagan and T. Zuchner, “Lanthanide-based time-resolved luminescence immunoassays,” *Anal Bioanal Chem*, vol. 400, no. 9, pp. 2847–2864, Jul. 2011, doi: 10.1007/s00216-011-5047-7.
[52] M. M. Attwood, D. Fabbro, A. V. Sokolov, S. Knapp, and H. B. Schiöth, “Trends in kinase drug discovery: targets, indications and inhibitor design,” *Nat Rev Drug Discov*, Aug. 2021, doi: 10.1038/s41573-021-00252-y.
[53] C. A. Lipinski, F. Lombardo, B. W. Dominy, and P. J. Feeney, “Experimental and computational approaches to estimate solubility and permeability in drug discovery and development settings,” *Advanced Drug Delivery Reviews*, vol. 23, no. 1–3, pp. 3–25, Jan. 1997, doi: 10.1016/S0169-409X(96)00423-1.
[54] R. Roskoski, “Classification of small molecule protein kinase inhibitors based upon the structures of their drug-enzyme complexes,” *Pharmacological Research*, vol. 103, pp. 26–48, Jan. 2016, doi: 10.1016/j.phrs.2015.10.021.
[55] C. H. Arrowsmith *et al.*, “The promise and peril of chemical probes,” *Nat Chem Biol*, vol. 11, no. 8, pp. 536–541, Aug. 2015, doi: 10.1038/nchembio.1867.
[56] K. Huang and A. A. Martí, “Optimizing the Sensitivity of Photoluminescent Probes Using Time-Resolved Spectroscopy: A Molecular Beacon Case Study,” *Anal. Chem.*, vol. 84, no. 18, pp. 8075–8082, Sep. 2012, doi: 10.1021/ac3019894.
[57] A. Lochner and J. A. Moolman, “The Many Faces of H89: A Review,” *Cardiovascular Drug Reviews*, vol. 24, no. 3–4, pp. 261–274, Sep. 2006, doi: 10.1111/j.1527-3466.2006.00261.x.
[58] F. Cervantes-Gomez, B. Lavergne, M. J. Keating, W. G. Wierda, and V. Gandhi, “Combination of Pim kinase inhibitors and Bcl-2 antagonists in chronic lymphocytic leukemia cells,” *Leukemia & Lymphoma*, vol. 57, no. 2, pp. 436–444, Feb. 2016, doi: 10.3109/10428194.2015.1063141.
[59] Z. A. Knight and K. M. Shokat, “Features of selective kinase inhibitors,” *Chem. Biol.*, vol. 12, no. 6, pp. 621–637, Jun. 2005, doi: 10.1016/j.chembiol.2005.04.011.
[60] H. Kaplon and J. M. Reichert, “Antibodies to watch in 2019,” *MAbs*, vol. 11, no. 2, pp. 219–238, Mar. 2019, doi: 10.1080/19420862.2018.1556465.
[61] T. Lopez *et al.*, “Functional selection of protease inhibitory antibodies,” *Proc Natl Acad Sci USA*, vol. 116, no. 33, pp. 16314–16319, Aug. 2019, doi: 10.1073/pnas.1903330116.

[62] F. Traincard, V. Giacomoni, and M. Veron, “Specific inhibition of AGC protein kinases by antibodies against C-terminal epitopes,” *FEBS Letters*, vol. 572, no. 1–3, pp. 276–280, Aug. 2004, doi: 10.1016/j.febslet.2004.07.013.
[63] K. L. Leach, E. A. Powers, J. C. McGuire, L. Dong, S. C. Kiley, and S. Jaken, “Monoclonal antibodies specific for type 3 protein kinase C recognize distinct domains of protein kinase C and inhibit in vitro functional activity,” *J. Biol. Chem.*, vol. 263, no. 26, pp. 13223–13230, Sep. 1988.
[64] Y. Chen and B. L. Sabatini, “The Kinase Specificity of Protein Kinase Inhibitor Peptide,” *Front Pharmacol*, vol. 12, p. 632815, 2021, doi: 10.3389/fphar.2021.632815.
[65] D. B. Glass, H.-C. Cheng, L. Mende-Mueller, J. Reed, and D. A. Walsh, “Primary structural determinants essential for potent inhibition of cAMP-dependent protein kinase by inhibitory peptides corresponding to the active portion of the heat-stable inhibitor protein,” *J. Biol. Chem.*, vol. 264, p. 8802, 1989.
[66] R. Kivi, P. Jemth, and J. Järv, “Thermodynamic Aspects of cAMP Dependent Protein Kinase Catalytic Subunit Allostery,” *Protein J*, vol. 33, no. 4, pp. 386–393, Aug. 2014, doi: 10.1007/s10930-014-9570-1.
[67] R. Ekambaram *et al.*, “Selective Bisubstrate Inhibitors with Sub-nanomolar Affinity for Protein Kinase Pim-1,” *ChemMedChem*, vol. 8, no. 6, pp. 909–913, Jun. 2013, doi: 10.1002/cmdc.201300042.
[68] J. R. Nair *et al.*, “Novel inhibition of PIM2 kinase has significant anti-tumor efficacy in multiple myeloma,” *Leukemia*, vol. 31, no. 8, pp. 1715–1726, Aug. 2017, doi: 10.1038/leu.2016.379.
[69] A. Casimiro-Garcia *et al.*, “Identification of Cyanamide-Based Janus Kinase 3 (JAK3) Covalent Inhibitors,” *J. Med. Chem.*, vol. 61, no. 23, pp. 10665–10699, Dec. 2018, doi: 10.1021/acs.jmedchem.8b01308.
[70] R. Roskoski, “Orally effective FDA-approved protein kinase targeted covalent inhibitors (TCIs),” *Pharmacol Res*, vol. 165, p. 105422, Mar. 2021, doi: 10.1016/j.phrs.2021.105422.
[71] R. A. Coover *et al.*, “Design, synthesis, and in vitro evaluation of a fluorescently labeled irreversible inhibitor of the catalytic subunit of cAMP-dependent protein kinase (PKACα),” *Org. Biomol. Chem.*, vol. 14, no. 20, pp. 4576–4581, 2016, doi: 10.1039/C6OB00529B.
[72] D. Lavogina, E. Enkvist, and A. Uri, “Bisubstrate Inhibitors of Protein Kinases: from Principle to Practical Applications,” *ChemMedChem*, vol. 5, no. 1, pp. 23–34, Jan. 2010, doi: 10.1002/cmdc.200900252.
[73] A. Ricouart, J. C. Gesquiere, A. Tartar, and C. Sergheraert, “Design of potent protein kinases inhibitors using the bisubstrate approach,” *J. Med. Chem.*, vol. 34, no. 1, pp. 73–78, Jan. 1991, doi: 10.1021/jm00105a012.
[74] D. Lavogina *et al.*, “Structural Analysis of ARC-Type Inhibitor (ARC-1034) Binding to Protein Kinase A Catalytic Subunit and Rational Design of Bisubstrate Analogue Inhibitors of Basophilic Protein Kinases,” *Journal of Medicinal Chemistry*, vol. 52, no. 2, pp. 308–321, Jan. 2009, doi: 10.1021/jm800797n.
[75] A. Pflug *et al.*, “Diversity of Bisubstrate Binding Modes of Adenosine Analogue–Oligoarginine Conjugates in Protein Kinase A and Implications for Protein Substrate Interactions,” *Journal of Molecular Biology*, vol. 403, no. 1, pp. 66–77, Oct. 2010, doi: 10.1016/j.jmb.2010.08.028.

[76] T. Ivan *et al.*, “Bifunctional Ligands for Inhibition of Tight-Binding Protein–Protein Interactions,” *Bioconjugate Chemistry*, vol. 27, no. 8, pp. 1900–1910, Aug. 2016, doi: 10.1021/acs.bioconjchem.6b00293.

[77] A. Vaasa *et al.*, “High-affinity bisubstrate probe for fluorescence anisotropy binding/displacement assays with protein kinases PKA and ROCK,” *Analytical Biochemistry*, vol. 385, no. 1, pp. 85–93, Feb. 2009, doi: 10.1016/j.ab.2008.10.030.

[78] D. Lavogina *et al.*, “Conjugates of 5-isoquinolinesulfonylamides and oligo-d-arginine possess high affinity and selectivity towards Rho kinase (ROCK),” *Bioorganic & Medicinal Chemistry Letters*, vol. 22, no. 10, pp. 3425–3430, May 2012, doi: 10.1016/j.bmcl.2012.03.101.

[79] E. Enkvist *et al.*, “Protein-Induced Long Lifetime Luminescence of Nonmetal Probes,” *ACS Chemical Biology*, vol. 6, no. 10, pp. 1052–1062, Oct. 2011, doi: 10.1021/cb200120v.

[80] H. Sinijarv, S. Wu, T. Ivan, T. Laasfeld, K. Viht, and A. Uri, “Binding assay for characterization of protein kinase inhibitors possessing sub-picomolar to sub-millimolar affinity,” *Analytical Biochemistry*, vol. 531, pp. 67–77, Aug. 2017.

[81] C. J. Hastie, H. J. McLauchlan, and P. Cohen, “Assay of protein kinases using radiolabeled ATP: a protocol,” *Nat Protoc*, vol. 1, no. 2, pp. 968–971, Aug. 2006, doi: 10.1038/nprot.2006.149.

[82] K. Viht, A. Vaasa, G. Raidaru, E. Enkvist, and A. Uri, “Fluorometric TLC assay for evaluation of protein kinase inhibitors,” *Analytical Biochemistry*, vol. 340, no. 1, pp. 165–170, May 2005, doi: 10.1016/j.ab.2005.02.008.

[83] J. J. Witt and R. Roskoski, “Rapid protein kinase assay using phosphocellulose-paper absorption,” *Analytical Biochemistry*, vol. 66, no. 1, pp. 253–258, May 1975, doi: 10.1016/0003-2697(75)90743-5.

[84] N. M. Luzi, C. E. Lyons, D. L. Peterson, and K. C. Ellis, “Characterization of PKACα enzyme kinetics and inhibition in an HPLC assay with a chromophoric substrate,” *Anal. Biochem.*, vol. 532, pp. 45–52, 01 2017, doi: 10.1016/j.ab.2017.06.001.

[85] H. Ma, K. Y. Horiuchi, Y. Wang, S. A. Kucharewicz, and S. L. Diamond, “Nanoliter Homogenous Ultra-High Throughput Screening Microarray for Lead Discoveries and IC_{50} Profiling,” *ASSAY and Drug Development Technologies*, vol. 3, no. 2, pp. 177–187, Apr. 2005, doi: 10.1089/adt.2005.3.177.

[86] K. Viht *et al.*, “Surface-plasmon-resonance-based biosensor with immobilized bisubstrate analog inhibitor for the determination of affinities of ATP- and protein-competitive ligands of cAMP-dependent protein kinase,” *Analytical Biochemistry*, vol. 362, no. 2, pp. 268–277, Mar. 2007, doi: 10.1016/j.ab.2006.12.041.

[87] J. C. Owicki, “Fluorescence polarization and anisotropy in high throughput screening: perspectives and primer,” *J Biomol Screen*, vol. 5, no. 5, pp. 297–306, Oct. 2000, doi: 10.1177/108705710000500501.

[88] K. S. Khatri, P. Modi, S. Sharma, and S. Deep, “Thermodynamics of Protein-Ligand Binding,” in *Frontiers in Protein Structure, Function, and Dynamics*, D. B. Singh and T. Tripathi, Eds. Singapore: Springer Singapore, 2020, pp. 145–185. doi: 10.1007/978-981-15-5530-5_7.

[89] G. G. Ferenczy and G. M. Keserű, “Thermodynamic profiling for fragment-based lead discovery and optimization,” *Expert Opinion on Drug Discovery*, vol. 15, no. 1, pp. 117–129, Jan. 2020, doi: 10.1080/17460441.2020.1691166.

[90] A. Assadieskandar *et al.*, “Effects of rigidity on the selectivity of protein kinase inhibitors,” *European Journal of Medicinal Chemistry*, vol. 146, pp. 519–528, Feb. 2018, doi: 10.1016/j.ejmech.2018.01.053.

[91] K. McAulay *et al.*, “Alkynyl Benzoxazines and Dihydroquinazolines as Cysteine Targeting Covalent Warheads and Their Application in Identification of Selective Irreversible Kinase Inhibitors,” *J. Am. Chem. Soc.*, vol. 142, no. 23, pp. 10358–10372, Jun. 2020, doi: 10.1021/jacs.9b13391.

[92] S. X. Leng, J. E. McElhaney, J. D. Walston, D. Xie, N. S. Fedarko, and G. A. Kuchel, “ELISA and Multiplex Technologies for Cytokine Measurement in Inflammation and Aging Research,” *The Journals of Gerontology Series A: Biological Sciences and Medical Sciences*, vol. 63, no. 8, pp. 879–884, Aug. 2008, doi: 10.1093/gerona/63.8.879.

[93] D. M. Rissin *et al.*, “Simultaneous detection of single molecules and singulated ensembles of molecules enables immunoassays with broad dynamic range,” *Anal. Chem.*, vol. 83, no. 6, pp. 2279–2285, Mar. 2011, doi: 10.1021/ac103161b.

[94] Y. Zhang *et al.*, “Development of a double monoclonal antibody–based sandwich enzyme-linked immunosorbent assay for detecting canine distemper virus,” *Appl Microbiol Biotechnol*, vol. 104, no. 24, pp. 10725–10735, Dec. 2020, doi: 10.1007/s00253-020-10997-y.

[95] C.-S. Chen and H. Zhu, “Protein Microarrays,” *BioTechniques*, vol. 40, no. 4, pp. 423–429, Apr. 2006, doi: 10.2144/06404TE01.

[96] W. Kusnezow *et al.*, “Optimal Design of Microarray Immunoassays to Compensate for Kinetic Limitations: Theory and Experiment,” *Molecular & Cellular Proteomics*, vol. 5, no. 9, pp. 1681–1696, Sep. 2006, doi: 10.1074/mcp.T500035-MCP200.

[97] C. Nitsche and G. Otting, “NMR studies of ligand binding,” *Current Opinion in Structural Biology*, vol. 48, pp. 16–22, Feb. 2018, doi: 10.1016/j.sbi.2017.09.001.

[98] K. C. Qian *et al.*, “Structural Basis of Constitutive Activity and a Unique Nucleotide Binding Mode of Human Pim-1 Kinase,” *J. Biol. Chem.*, vol. 280, no. 7, pp. 6130–6137, Feb. 2005, doi: 10.1074/jbc.M409123200.

[99] J. Yang *et al.*, “Contribution of non-catalytic core residues to activity and regulation in protein kinase A,” *J. Biol. Chem.*, vol. 284, p. 6241, 2009.

[100] M. Kasari *et al.*, “Responsive microsecond-lifetime photoluminescent probes for analysis of protein kinases and their inhibitors,” *Biochimica et Biophysica Acta (BBA) - Proteins and Proteomics*, vol. 1834, no. 7, pp. 1330–1335, Jul. 2013, doi: 10.1016/j.bbapap.2013.02.039.

[101] W. Kabsch, “*XDS*,” *Acta Crystallogr D Biol Crystallogr*, vol. 66, no. 2, pp. 125–132, Feb. 2010, doi: 10.1107/S0907444909047337.

[102] P. R. Evans and G. N. Murshudov, “How good are my data and what is the resolution?,” *Acta Crystallogr D Biol Crystallogr*, vol. 69, no. 7, pp. 1204–1214, Jul. 2013, doi: 10.1107/S0907444913000061.

[103] A. J. McCoy, R. W. Grosse-Kunstleve, P. D. Adams, M. D. Winn, L. C. Storoni, and R. J. Read, “*Phaser* crystallographic software,” *J Appl Crystallogr*, vol. 40, no. 4, pp. 658–674, Aug. 2007, doi: 10.1107/S0021889807021206.

[104] O. Fedorov *et al.*, “A systematic interaction map of validated kinase inhibitors with Ser/Thr kinases,” *Proceedings of the National Academy of Sciences*, vol. 104, no. 51, pp. 20523–20528, Dec. 2007, doi: 10.1073/pnas.0708800104.

[105] P. Emsley and M. Crispin, “Structural analysis of glycoproteins: building N-linked glycans with *Coot*,” *Acta Crystallogr D Struct Biol*, vol. 74, no. 4, pp. 256–263, Apr. 2018, doi: 10.1107/S2059798318005119.

[106] O. Kovalevskiy, R. A. Nicholls, F. Long, A. Carlon, and G. N. Murshudov, “Overview of refinement procedures within *REFMAC* 5: utilizing data from different sources,” *Acta Crystallogr D Struct Biol*, vol. 74, no. 3, pp. 215–227, Mar. 2018, doi: 10.1107/S2059798318000979.

[107] D. Lavogina *et al.*, “Adenosine analogue–oligo-arginine conjugates (ARCs) serve as high-affinity inhibitors and fluorescence probes of type I cGMP-dependent protein kinase (PKGIα),” *Biochimica et Biophysica Acta (BBA) - Proteins and Proteomics*, vol. 1804, no. 9, pp. 1857–1868, Sep. 2010, doi: 10.1016/j.bbapap.2010.04.007.

[108] P. Chames, M. Van Regenmortel, E. Weiss, and D. Baty, “Therapeutic antibodies: successes, limitations and hopes for the future,” *Br J Pharmacol*, vol. 157, no. 2, pp. 220–233, May 2009, doi: 10.1111/j.1476-5381.2009.00190.x.

[109] Y. N. Abdiche *et al.*, “Antibodies Targeting Closely Adjacent or Minimally Overlapping Epitopes Can Displace One Another,” *PLoS ONE*, vol. 12, no. 1, p. e0169535, Jan. 2017, doi: 10.1371/journal.pone.0169535.

[110] P. Akamine, W. Madhusudan J., N. H. Xuong, L. F. Ten Eyck, and S. S. Taylor, “Dynamic features of cAMP-dependent protein kinase revealed by apoenzyme crystal structure,” *J. Mol. Biol.*, vol. 327, p. 159, 2003.

[111] G. D. Dalton and W. L. Dewey, “Protein kinase inhibitor peptide (PKI): A family of endogenous neuropeptides that modulate neuronal cAMP-dependent protein kinase function,” *Neuropeptides*, vol. 40, no. 1, pp. 23–34, Feb. 2006, doi: 10.1016/j.npep.2005.10.002.

[112] V. Raghuram, K. Salhadar, K. Limbutara, E. Park, C.-R. Yang, and M. A. Knepper, “Protein kinase A catalytic-α and catalytic-β proteins have non-redundant functions,” Systems Biology, preprint, Jul. 2020. doi: 10.1101/2020.07.01.182691.

[113] C. Breitenlechner *et al.*, “Protein kinase A in complex with Rho-kinase inhibitors Y-27632, Fasudil, and H-1152P: structural basis of selectivity,” *Structure*, vol. 11, no. 12, pp. 1595–1607, Dec. 2003, doi: 10.1016/j.str.2003.11.002.

[114] D. I. Kisiela *et al.*, “Inhibition and Reversal of Microbial Attachment by an Antibody with Parasteric Activity against the FimH Adhesin of Uropathogenic E. coli,” *PLoS Pathog*, vol. 11, no. 5, p. e1004857, May 2015, doi: 10.1371/journal.ppat.1004857.

[115] K. Pyo, V. D. Thanthirige, K. Kwak, P. Pandurangan, G. Ramakrishna, and D. Lee, “Ultrabright Luminescence from Gold Nanoclusters: Rigidifying the Au(I)–Thiolate Shell,” *J. Am. Chem. Soc.*, vol. 137, no. 25, pp. 8244–8250, Jul. 2015, doi: 10.1021/jacs.5b04210.

[116] S. M. Borisov, “CHAPTER 1. Fundamentals of Quenched Phosphorescence O2 Sensing and Rational Design of Sensor Materials,” in *Detection Science*, D. B. Papkovsky and R. I. Dmitriev, Eds. Cambridge: Royal Society of Chemistry, 2018, pp. 1–18. doi: 10.1039/9781788013451-00001.

[117] L. Prade, R. A. Engh, A. Girod, V. Kinzel, R. Huber, and D. Bossemeyer, “Staurosporine-induced conformational changes of cAMP-dependent protein kinase catalytic subunit explain inhibitory potential,” *Structure*, vol. 5, no. 12, pp. 1627–1637, Dec. 1997, doi: 10.1016/S0969-2126(97)00310-9.

[118] J. Guergnon *et al.*, "A PKA survival pathway inhibited by DPT-PKI, a new specific cell permeable PKA inhibitor, is induced by T. annulata in parasitized B-lymphocytes," *Apoptosis*, vol. 11, no. 8, pp. 1263–1273, Aug. 2006, doi: 10.1007/s10495-006-7702-6.

[119] D. A. Heerding *et al.*, "Identification of 4-(2-(4-Amino-1,2,5-oxadiazol-3-yl)-1-ethyl-7-{[(3 *S*)-3-piperidinylmethyl]oxy}-1 *H* -imidazo[4,5- *c*]pyridin-4-yl)-2-methyl-3-butyn-2-ol (GSK690693), a Novel Inhibitor of AKT Kinase," *J. Med. Chem.*, vol. 51, no. 18, pp. 5663–5679, Sep. 2008, doi: 10.1021/jm8004527.

[120] N. M. Luzi, C. E. Lyons, D. L. Peterson, and K. C. Ellis, "Kinetics and inhibition studies of the L205R mutant of cAMP-dependent protein kinase involved in Cushing's syndrome," *FEBS Open Bio*, vol. 8, no. 4, pp. 606–613, Apr. 2018, doi: 10.1002/2211-5463.12396.

[121] R. Ekambaram *et al.*, "Selective Bisubstrate Inhibitors with Sub-nanomolar Affinity for Protein Kinase Pim-1," *ChemMedChem*, vol. 8, no. 6, pp. 909–913, Jun. 2013, doi: 10.1002/cmdc.201300042.

[122] Z.-F. Tao *et al.*, "Discovery of 3 *H* -Benzo[4,5]thieno[3,2- *d*]pyrimidin-4-ones as Potent, Highly Selective, and Orally Bioavailable Inhibitors of the Human Protooncogene Proviral Insertion Site in Moloney Murine Leukemia Virus (PIM) Kinases," *J. Med. Chem.*, vol. 52, no. 21, pp. 6621–6636, Nov. 2009, doi: 10.1021/jm900943h.

[123] V. Pogacic *et al.*, "Structural Analysis Identifies Imidazo[1,2- *b*]Pyridazines as PIM Kinase Inhibitors with *In vitro* Antileukemic Activity," *Cancer Res*, vol. 67, no. 14, pp. 6916–6924, Jul. 2007, doi: 10.1158/0008-5472.CAN-07-0320.

[124] K. Tsuganezawa *et al.*, "A Novel Pim-1 Kinase Inhibitor Targeting Residues That Bind the Substrate Peptide," *Journal of Molecular Biology*, vol. 417, no. 3, pp. 240–252, Mar. 2012, doi: 10.1016/j.jmb.2012.01.036.

[125] A. Vaasa, M. Lust, A. Terrin, A. Uri, and M. Zaccolo, "Small-molecule FRET probes for protein kinase activity monitoring in living cells," *Biochemical and Biophysical Research Communications*, vol. 397, no. 4, pp. 750–755, Jul. 2010, doi: 10.1016/j.bbrc.2010.06.026.

[126] C. W. Tornøe, C. Christensen, and M. Meldal, "Peptidotriazoles on Solid Phase: [1,2,3]-Triazoles by Regiospecific Copper(I)-Catalyzed 1,3-Dipolar Cycloadditions of Terminal Alkynes to Azides," *J. Org. Chem.*, vol. 67, no. 9, pp. 3057–3064, May 2002, doi: 10.1021/jo011148j.

[127] M. Berna and B. Ackermann, "Increased throughput for low-abundance protein biomarker verification by liquid chromatography/tandem mass spectrometry," *Anal Chem*, vol. 81, no. 10, pp. 3950–3956, May 2009, doi: 10.1021/ac9002744.

[128] L. Chang *et al.*, "Single molecule enzyme-linked immunosorbent assays: Theoretical considerations," *Journal of Immunological Methods*, vol. 378, no. 1–2, pp. 102–115, Apr. 2012, doi: 10.1016/j.jim.2012.02.011.

[129] W. Kusnezow *et al.*, "Optimal Design of Microarray Immunoassays to Compensate for Kinetic Limitations: Theory and Experiment," *Molecular & Cellular Proteomics*, vol. 5, no. 9, pp. 1681–1696, Sep. 2006, doi: 10.1074/mcp.T500035-MCP200.

[130] R. Walker-Gray, F. Stengel, and M. G. Gold, "Mechanisms for restraining cAMP-dependent protein kinase revealed by subunit quantitation and cross-linking approaches," *Proceedings of the National Academy of Sciences*, vol. 114, no. 39, pp. 10414–10419, Sep. 2017, doi: 10.1073/pnas.1701782114.

[131] A. Saeed, R. Wang, S. Ling, and S. Wang, “Antibody Engineering for Pursuing a Healthier Future,” *Front Microbiol*, vol. 8, p. 495, 2017, doi: 10.3389/fmicb.2017.00495.

[132] J. Vahter, K. Viht, A. Uri, G. babu Manoharan, and E. Enkvist, “Thiazole- and selenazole-comprising high-affinity inhibitors possess bright microsecond-scale photoluminescence in complex with protein kinase CK2,” *Bioorganic & Medicinal Chemistry*, vol. 26, no. 18, pp. 5062–5068, Oct. 2018, doi: 10.1016/j.bmc.2018.09.003.

[133] Y. Wang, J. Xiu, C. Ren, and Z. Yu, “Protein kinase PIM2: A simple PIM family kinase with complex functions in cancer metabolism and therapeutics,” *J. Cancer*, vol. 12, no. 9, pp. 2570–2581, 2021, doi: 10.7150/jca.53134.

[134] E. F. Douglass, C. J. Miller, G. Sparer, H. Shapiro, and D. A. Spiegel, “A Comprehensive Mathematical Model for Three-Body Binding Equilibria,” *Journal of the American Chemical Society*, vol. 135, no. 16, pp. 6092–6099, Apr. 2013, doi: 10.1021/ja311795d.

[135] V. Navrátil *et al.*, “DNA-linked Inhibitor Antibody Assay (DIANA) for sensitive and selective enzyme detection and inhibitor screening,” *Nucleic Acids Res*, vol. 45, no. 2, p. e10, Jan. 2017, doi: 10.1093/nar/gkw853.

[136] N. M. Santio *et al.*, “Phosphorylation of Notch1 by Pim kinases promotes oncogenic signaling in breast and prostate cancer cells,” *Oncotarget*, vol. 7, no. 28, pp. 43220–43238, Jul. 2016, doi: 10.18632/oncotarget.9215.

SUMMARY IN ESTONIAN

Inhibiitorid ja fotoluminestsents-sondid proteiinkinaaside PKA ja PIM *in vitro* uuringuteks

Proteiinkinaasid katalüüsivad valkude fosforüülimist, fosfaatrühma ülekannet ATP-lt sihtvalkudele. Proteiinkinaaside normaalsest erinev aktiivsus rakkudes võib olla selliste komplekssete haiguste, nagu vähktõbi, diabeet ja südame-veresoonkonna haigused, põhjuseks või tunnuseks. Sellest tulenevalt teeb farmaatsiatööstus märkimisväärseid jõupingutusi proteiinkinaaside aktiivsuse reguleerimiseks inhibiitoritega ning nende ensüümide aktiivsuse jälgimiseks luminestsentssondidega. Nende eesmärkide saavutamiseks arendatakse erineva keemilise struktuuriga aineid, väikestest orgaanilistest molekulidest inhibeerivate antikehadeni. Viimase veerandsajandi jooksul on ravimiturule jõudnud üle 70 ravimi, mis mõjutavad proteiinkinaaside aktiivsust rakkudes.

Käesolevas töös kasutatud ARC-inhibiitorid on keemiliselt struktuurilt adenosiini matkivate heteroaromaatsete fragmentide ja peptiidide analoogide konjugaadid, neid ühendeid on pikemalt uuritud Tartu Ülikooli keemia instituudis. Kasutades uurimisgrupis varem konstrueeritud ARC-Lum(Fluo) fotoluminestsents-sonde näidati käesolevas uurimistöös, et proteiinkinaasi PKA katalüütilise alaühiku α-isovormi (PKAcα) monoklonaalse antikeha (kloon D38C6) seondumine sihtvalguga on konkurentne ARC-Lum(Fluo) sondi seondumisega. Seejärel selgus, et mAb(D38C6) pärsib kinaasi fosforüülimisaktiivsust madala nanomolaarse inhibeeriva toimega (K_i = 2,4 nM). Nimetatud antikeha omadus tuleneb sellest, et mAb(D38C6) ja ARC-inhibiitorid (aga ka ATP) seonduvad kahe erineva PKAcα konformeeriga. Nende võistlevate PKAcα ligandidega [mAb(D38C6) ja ARC] järjestikust töötlemist kasutati tundliku AbARC immuunanalüüsi meetodi arendamiseks, mis võimaldas määrata PKAcα väikeseid koguseid (alates 93 pg) rakulüsaatides.

Hiljuti avastati Cushingi sündroomiga patsiendil S54L mutatsiooniga *PRKACB* geen. See mutatsioon viib proteiinkinaasi glütsiinirikka aasa struktuuri muutuseni. Käesoleva uuringu käigus arendati inhibiitor, millel on selle muteerunud proteiinkinaasi suhtes kuuekordne selektiivsus. Lisaks töötati välja luminestsentsmeetod, mis võimaldab määrata nii turustatavate kui ka arendatavate inhibiitorite afiinsusi PKAcβ valgu suhtes. Uusi fotoluminestsentssonde kasutati ka S54L mutatsiooni tulemusena PKAcβ-valgus toimuvate konformatsiooniliste ümberkorralduste uurimiseks.

Koostöös Oxfordi ülikooliga viidi läbi ARC-inhibiitorite ja proteiinkinaasi PIM-1 komplekside röntgenstruktuuranalüüs. Saadud struktuurimudelitest lähtuvalt konstrueeriti lihtsustatud keemilise ehitusega ained. Uued inhibiitorid säilitasid madala nanomolaarse toime ja nende mõju oli selektiivne PIM-kinaaside suhtes. Inhibiitorite märgistamisel fluorestsentsvärvidega saadi PIM-selektiivsed fluorestsents-sondid, mis läbisid hästi rakkude plasmamembraane. Elusrakkude konfokaalmikroskoopia selgitas ARC-sondide jaotuse rakus, mis kattus transfekteeritud fluorestsentsvalgu ja PIM-1 liitvalgu paiknemisega.

Samuti kasutati uusi inhibiitoreid kombinatsioonis PIM-2-spetsiifiliste antikehadega vähi biomarkerite testi AbARC-2 väljatöötamiseks.

Selles töös konstrueeritud inhibiitorid ja fluorestsents-sondid on mitmekülgsed keemilised vahendeid proteinkinaaside PKAc ja PIM funktsioonide selgitamiseks normaalsetes ja haigusliku füsioloogiaga rakkudes.

ACKNOWLEDGEMENTS

First, I like to thank all the people, who has devoted their time and knowledge to help me get this far in research.

I would like to express my gratitude to my supervisor Asko Uri for taking me into your research group and introducing me to a new field of science. Thank you for the supervision, guidance, and all the interesting and encouraging conversations about protein kinases, their inhibitors, and technologies in general during all these years. My gratitude to my second supervisor Erki Enkvist for everything you taught me, and for your view on the nature. I am very thankful to Kaido Viht for teaching me the methodology of working with protein kinases and for being present during these years. Darja Lavõgina, if these cells could talk, they would thank you better than me. Thank you for the many experience-based tips during these years. I enjoyed the company of Jürgen, Katrin, and Tanel, who had to put up with me for years. I also wish to thank everybody else in the Chair of Bioorganic Chemistry especially the scientists in the Medicinal chemistry workgroup and my different co-authors.

I want to thank my big family for their support, especially my spouse Grâce who has been the most important person in my life, with whom I have a beautiful baby girl, Maïsha. Dad wants you at this level someday. My gratitude goes to my late father Sébastien Nonga, doctor in Organic chemistry, for putting me on the right track. This work is dedicated to you, up there!

Finally, I want to express my deepest gratitude to my friends at the Church of Immaculate Conception of the Blessed Virgin Mary and YliCool Basketball club, especially Gunnar, Karel, Indrek, Marek, Helari, Arnis, Gratian, Daiga, Kaaleb, Innocent, Gabriela, and Georg Elias. We went through tough times together!

PUBLICATIONS

CURRICULUM VITAE

Name: Olivier Etebe Nonga
Date of Birth: April 21, 1990
Citizenship: Congolese
Address: University of Tartu, Institute of Chemistry, Ravila 14a, 50411, Tartu, Estonia
e-mail: olivier.etebe.nonga@ut.ee

Education

2017–2021 University of Tartu, PhD student in chemistry
2015–2017 University of Tartu, MSc in chemistry
2011–2015 Voronezh State University, BSc in chemistry

Professional self-improvement

- 2019 10th Inhibitors of Protein Kinases Conference, Warsaw, Poland (14th–19th September 2019)
- 2019 Summer school – Basics to work with Extracellular Vesicles, Tartu, Estonia (23rd–25th May 2019)

Scientific publications

1. **O. E. Nonga**, D. Lavogina, E. Enkvist, K. Kestav, A. Chaikuad, S. E. Dixon-Clarke, A. N. Bullock, S. Kopanchuk, T. Ivan, R. Ekambaram, K. Viht, S. Knapp, and A. Uri, "Crystal structure-guided design of bisubstrate inhibitors and photoluminescent probes for protein kinases of the PIM family," *Molecules*, vol. 26 , no. 14, pp. 4353, Jul. 2021.
2. **O. E. Nonga**, E. Enkvist, F. W. Herberg, and A. Uri, "Inhibitors and fluorescent probes for protein kinase PKAcβ and its S54L mutant, identified in a patient with cortisol producing adenoma," *Bioscience, Biotechnology, and Biochemistry*, vol. 84, no. 9, pp. 1839–1845, Sep. 2020.
3. **O. E. Nonga**, D. Lavogina, T. Ivan, K. Viht, E. Enkvist, and A. Uri, "Discovery of strong inhibitory properties of a monoclonal antibody of PKA and use of the antibody and a competitive photoluminescent orthosteric probe for analysis of the protein kinase," *Biochimica et Biophysica Acta (BBA) – Proteins and Proteomics*, vol. 1868, no. 8, p. 140427, Aug. 2020.
4. A. Uri and **O. E. Nonga**, "What is the current value of fluorescence polarization assays in small molecule screening?," *Expert Opinion on Drug Discovery*, vol. 15, no. 2, pp. 131–133, Feb. 2020.

ELULOOKIRJELDUS

Nimi: Olivier Etebe Nonga
Sünniaeg: Aprill 7, 1990
Kodakondsus: Kongo
Aadress: Tartu Ülikool, keemia instituut, Ravila 14a, 50411, Tartu, Eesti
E-mail: olivier.etebe.nonga@ut.ee

Hariduskäik

2017–2021 Tartu Ülikool, doktoriõpe keemias
2015–2017 Tartu Ülikool, MSc keemias
2011–2015 Voroneži Riiklik Ülikool, BSc keemias

Erialane enesetäiendus

- 2019 Konverents – 10th Inhibitors of Protein Kinases, Varssavi, Poola (14–19 September 2019)
- 2019 Suvekool – Basics to work with Extracellular Vesicles, Tartu, Eesti (23–25 Mai 2019)

Teaduspublikatsioonid

1. **O. E. Nonga**, D. Lavogina, E. Enkvist, K. Kestav, A. Chaikuad, S. E. Dixon-Clarke, A. N. Bullock, S. Kopanchuk, T. Ivan, R. Ekambaram, K. Viht, S. Knapp, and A. Uri, "Crystal structure-guided design of bisubstrate inhibitors and photoluminescent probes for protein kinases of the PIM family," *Molecules*, vol. 26 , no. 14, pp. 4353, Jul. 2021.
2. **O. E. Nonga**, E. Enkvist, F. W. Herberg, and A. Uri, "Inhibitors and fluorescent probes for protein kinase PKAcβ and its S54L mutant, identified in a patient with cortisol producing adenoma," *Bioscience, Biotechnology, and Biochemistry*, vol. 84, no. 9, pp. 1839–1845, Sep. 2020.
3. **O. E. Nonga**, D. Lavogina, T. Ivan, K. Viht, E. Enkvist, and A. Uri, "Discovery of strong inhibitory properties of a monoclonal antibody of PKA and use of the antibody and a competitive photoluminescent orthosteric probe for analysis of the protein kinase," *Biochimica et Biophysica Acta (BBA) – Proteins and Proteomics*, vol. 1868, no. 8, p. 140427, Aug. 2020.
4. A. Uri and **O. E. Nonga**, "What is the current value of fluorescence polarization assays in small molecule screening?," *Expert Opinion on Drug Discovery*, vol. 15, no. 2, pp. 131–133, Feb. 2020

DISSERTATIONES CHIMICAE UNIVERSITATIS TARTUENSIS

1. **Toomas Tamm.** Quantum-chemical simulation of solvent effects. Tartu, 1993, 110 p.
2. **Peeter Burk.** Theoretical study of gas-phase acid-base equilibria. Tartu, 1994, 96 p.
3. **Victor Lobanov.** Quantitative structure-property relationships in large descriptor spaces. Tartu, 1995, 135 p.
4. **Vahur Mäemets.** The ^{17}O and ^{1}H nuclear magnetic resonance study of H_2O in individual solvents and its charged clusters in aqueous solutions of electrolytes. Tartu, 1997, 140 p.
5. **Andrus Metsala.** Microcanonical rate constant in nonequilibrium distribution of vibrational energy and in restricted intramolecular vibrational energy redistribution on the basis of slater's theory of unimolecular reactions. Tartu, 1997, 150 p.
6. **Uko Maran.** Quantum-mechanical study of potential energy surfaces in different environments. Tartu, 1997, 137 p.
7. **Alar Jänes.** Adsorption of organic compounds on antimony, bismuth and cadmium electrodes. Tartu, 1998, 219 p.
8. **Kaido Tammeveski.** Oxygen electroreduction on thin platinum films and the electrochemical detection of superoxide anion. Tartu, 1998, 139 p.
9. **Ivo Leito.** Studies of Brønsted acid-base equilibria in water and non-aqueous media. Tartu, 1998, 101 p.
10. **Jaan Leis.** Conformational dynamics and equilibria in amides. Tartu, 1998, 131 p.
11. **Toonika Rinken.** The modelling of amperometric biosensors based on oxidoreductases. Tartu, 2000, 108 p.
12. **Dmitri Panov.** Partially solvated Grignard reagents. Tartu, 2000, 64 p.
13. **Kaja Orupõld.** Treatment and analysis of phenolic wastewater with microorganisms. Tartu, 2000, 123 p.
14. **Jüri Ivask.** Ion Chromatographic determination of major anions and cations in polar ice core. Tartu, 2000, 85 p.
15. **Lauri Vares.** Stereoselective Synthesis of Tetrahydrofuran and Tetrahydropyran Derivatives by Use of Asymmetric Horner-Wadsworth-Emmons and Ring Closure Reactions. Tartu, 2000, 184 p.
16. **Martin Lepiku.** Kinetic aspects of dopamine D_2 receptor interactions with specific ligands. Tartu, 2000, 81 p.
17. **Katrin Sak.** Some aspects of ligand specificity of P2Y receptors. Tartu, 2000, 106 p.
18. **Vello Pällin.** The role of solvation in the formation of iotsitch complexes. Tartu, 2001, 95 p.
19. **Katrin Kollist.** Interactions between polycyclic aromatic compounds and humic substances. Tartu, 2001, 93 p.

20. **Ivar Koppel.** Quantum chemical study of acidity of strong and superstrong Brønsted acids. Tartu, 2001, 104 p.
21. **Viljar Pihl.** The study of the substituent and solvent effects on the acidity of OH and CH acids. Tartu, 2001, 132 p.
22. **Natalia Palm.** Specification of the minimum, sufficient and significant set of descriptors for general description of solvent effects. Tartu, 2001, 134 p.
23. **Sulev Sild.** QSPR/QSAR approaches for complex molecular systems. Tartu, 2001, 134 p.
24. **Ruslan Petrukhin.** Industrial applications of the quantitative structure-property relationships. Tartu, 2001, 162 p.
25. **Boris V. Rogovoy.** Synthesis of (benzotriazolyl)carboximidamides and their application in relations with *N*- and *S*-nucleophyles. Tartu, 2002, 84 p.
26. **Koit Herodes.** Solvent effects on UV-vis absorption spectra of some solvatochromic substances in binary solvent mixtures: the preferential solvation model. Tartu, 2002, 102 p.
27. **Anti Perkson.** Synthesis and characterisation of nanostructured carbon. Tartu, 2002, 152 p.
28. **Ivari Kaljurand.** Self-consistent acidity scales of neutral and cationic Brønsted acids in acetonitrile and tetrahydrofuran. Tartu, 2003, 108 p.
29. **Karmen Lust.** Adsorption of anions on bismuth single crystal electrodes. Tartu, 2003, 128 p.
30. **Mare Piirsalu.** Substituent, temperature and solvent effects on the alkaline hydrolysis of substituted phenyl and alkyl esters of benzoic acid. Tartu, 2003, 156 p.
31. **Meeri Sassian.** Reactions of partially solvated Grignard reagents. Tartu, 2003, 78 p.
32. **Tarmo Tamm.** Quantum chemical modelling of polypyrrole. Tartu, 2003. 100 p.
33. **Erik Teinemaa.** The environmental fate of the particulate matter and organic pollutants from an oil shale power plant. Tartu, 2003. 102 p.
34. **Jaana Tammiku-Taul.** Quantum chemical study of the properties of Grignard reagents. Tartu, 2003. 120 p.
35. **Andre Lomaka.** Biomedical applications of predictive computational chemistry. Tartu, 2003. 132 p.
36. **Kostyantyn Kirichenko.** Benzotriazole – Mediated Carbon–Carbon Bond Formation. Tartu, 2003. 132 p.
37. **Gunnar Nurk.** Adsorption kinetics of some organic compounds on bismuth single crystal electrodes. Tartu, 2003, 170 p.
38. **Mati Arulepp.** Electrochemical characteristics of porous carbon materials and electrical double layer capacitors. Tartu, 2003, 196 p.
39. **Dan Cornel Fara.** QSPR modeling of complexation and distribution of organic compounds. Tartu, 2004, 126 p.
40. **Riina Mahlapuu.** Signalling of galanin and amyloid precursor protein through adenylate cyclase. Tartu, 2004, 124 p.

41. **Mihkel Kerikmäe.** Some luminescent materials for dosimetric applications and physical research. Tartu, 2004, 143 p.
42. **Jaanus Kruusma.** Determination of some important trace metal ions in human blood. Tartu, 2004, 115 p.
43. **Urmas Johanson.** Investigations of the electrochemical properties of polypyrrole modified electrodes. Tartu, 2004, 91 p.
44. **Kaido Sillar.** Computational study of the acid sites in zeolite ZSM-5. Tartu, 2004, 80 p.
45. **Aldo Oras.** Kinetic aspects of dATPαS interaction with $P2Y_1$ receptor. Tartu, 2004, 75 p.
46. **Erik Mölder.** Measurement of the oxygen mass transfer through the air-water interface. Tartu, 2005, 73 p.
47. **Thomas Thomberg.** The kinetics of electroreduction of peroxodisulfate anion on cadmium (0001) single crystal electrode. Tartu, 2005, 95 p.
48. **Olavi Loog.** Aspects of condensations of carbonyl compounds and their imine analogues. Tartu, 2005, 83 p.
49. **Siim Salmar.** Effect of ultrasound on ester hydrolysis in aqueous ethanol. Tartu, 2006, 73 p.
50. **Ain Uustare.** Modulation of signal transduction of heptahelical receptors by other receptors and G proteins. Tartu, 2006, 121 p.
51. **Sergei Yurchenko.** Determination of some carcinogenic contaminants in food. Tartu, 2006, 143 p.
52. **Kaido Tämm.** QSPR modeling of some properties of organic compounds. Tartu, 2006, 67 p.
53. **Olga Tšubrik.** New methods in the synthesis of multisubstituted hydrazines. Tartu. 2006, 183 p.
54. **Lilli Sooväli.** Spectrophotometric measurements and their uncertainty in chemical analysis and dissociation constant measurements. Tartu, 2006, 125 p.
55. **Eve Koort.** Uncertainty estimation of potentiometrically measured ph and pK_a values. Tartu, 2006, 139 p.
56. **Sergei Kopanchuk.** Regulation of ligand binding to melanocortin receptor subtypes. Tartu, 2006, 119 p.
57. **Silvar Kallip.** Surface structure of some bismuth and antimony single crystal electrodes. Tartu, 2006, 107 p.
58. **Kristjan Saal.** Surface silanization and its application in biomolecule coupling. Tartu, 2006, 77 p.
59. **Tanel Tätte.** High viscosity $Sn(OBu)_4$ oligomeric concentrates and their applications in technology. Tartu, 2006, 91 p.
60. **Dimitar Atanasov Dobchev**. Robust QSAR methods for the prediction of properties from molecular structure. Tartu, 2006, 118 p.
61. **Hannes Hagu**. Impact of ultrasound on hydrophobic interactions in solutions. Tartu, 2007, 81 p.
62. **Rutha Jäger.** Electroreduction of peroxodisulfate anion on bismuth electrodes. Tartu, 2007, 142 p.

63. **Kaido Viht.** Immobilizable bisubstrate-analogue inhibitors of basophilic protein kinases: development and application in biosensors. Tartu, 2007, 88 p.
64. **Eva-Ingrid Rõõm.** Acid-base equilibria in nonpolar media. Tartu, 2007, 156 p.
65. **Sven Tamp.** DFT study of the cesium cation containing complexes relevant to the cesium cation binding by the humic acids. Tartu, 2007, 102 p.
66. **Jaak Nerut.** Electroreduction of hexacyanoferrate(III) anion on Cadmium (0001) single crystal electrode. Tartu, 2007, 180 p.
67. **Lauri Jalukse.** Measurement uncertainty estimation in amperometric dissolved oxygen concentration measurement. Tartu, 2007, 112 p.
68. **Aime Lust.** Charge state of dopants and ordered clusters formation in CaF_2:Mn and CaF_2:Eu luminophors. Tartu, 2007, 100 p.
69. **Iiris Kahn**. Quantitative Structure-Activity Relationships of environmentally relevant properties. Tartu, 2007, 98 p.
70. **Mari Reinik.** Nitrates, nitrites, N-nitrosamines and polycyclic aromatic hydrocarbons in food: analytical methods, occurrence and dietary intake. Tartu, 2007, 172 p.
71. **Heili Kasuk.** Thermodynamic parameters and adsorption kinetics of organic compounds forming the compact adsorption layer at Bi single crystal electrodes. Tartu, 2007, 212 p.
72. **Erki Enkvist.** Synthesis of adenosine-peptide conjugates for biological applications. Tartu, 2007, 114 p.
73. **Svetoslav Hristov Slavov**. Biomedical applications of the QSAR approach. Tartu, 2007, 146 p.
74. **Eneli Härk.** Electroreduction of complex cations on electrochemically polished Bi(*hkl*) single crystal electrodes. Tartu, 2008, 158 p.
75. **Priit Möller.** Electrochemical characteristics of some cathodes for medium temperature solid oxide fuel cells, synthesized by solid state reaction technique. Tartu, 2008, 90 p.
76. **Signe Viggor.** Impact of biochemical parameters of genetically different pseudomonads at the degradation of phenolic compounds. Tartu, 2008, 122 p.
77. **Ave Sarapuu.** Electrochemical reduction of oxygen on quinone-modified carbon electrodes and on thin films of platinum and gold. Tartu, 2008, 134 p.
78. **Agnes Kütt.** Studies of acid-base equilibria in non-aqueous media. Tartu, 2008, 198 p.
79. **Rouvim Kadis.** Evaluation of measurement uncertainty in analytical chemistry: related concepts and some points of misinterpretation. Tartu, 2008, 118 p.
80. **Valter Reedo.** Elaboration of IVB group metal oxide structures and their possible applications. Tartu, 2008, 98 p.
81. **Aleksei Kuznetsov.** Allosteric effects in reactions catalyzed by the cAMP-dependent protein kinase catalytic subunit. Tartu, 2009, 133 p.

82. **Aleksei Bredihhin.** Use of mono- and polyanions in the synthesis of multisubstituted hydrazine derivatives. Tartu, 2009, 105 p.
83. **Anu Ploom.** Quantitative structure-reactivity analysis in organosilicon chemistry. Tartu, 2009, 99 p.
84. **Argo Vonk.** Determination of adenosine A_{2A}- and dopamine D_1 receptor-specific modulation of adenylate cyclase activity in rat striatum. Tartu, 2009, 129 p.
85. **Indrek Kivi.** Synthesis and electrochemical characterization of porous cathode materials for intermediate temperature solid oxide fuel cells. Tartu, 2009, 177 p.
86. **Jaanus Eskusson.** Synthesis and characterisation of diamond-like carbon thin films prepared by pulsed laser deposition method. Tartu, 2009, 117 p.
87. **Marko Lätt.** Carbide derived microporous carbon and electrical double layer capacitors. Tartu, 2009, 107 p.
88. **Vladimir Stepanov.** Slow conformational changes in dopamine transporter interaction with its ligands. Tartu, 2009, 103 p.
89. **Aleksander Trummal.** Computational Study of Structural and Solvent Effects on Acidities of Some Brønsted Acids. Tartu, 2009, 103 p.
90. **Eerold Vellemäe.** Applications of mischmetal in organic synthesis. Tartu, 2009, 93 p.
91. **Sven Parkel.** Ligand binding to 5-HT_{1A} receptors and its regulation by Mg^{2+} and Mn^{2+}. Tartu, 2010, 99 p.
92. **Signe Vahur.** Expanding the possibilities of ATR-FT-IR spectroscopy in determination of inorganic pigments. Tartu, 2010, 184 p.
93. **Tavo Romann**. Preparation and surface modification of bismuth thin film, porous, and microelectrodes. Tartu, 2010, 155 p.
94. **Nadežda Aleksejeva.** Electrocatalytic reduction of oxygen on carbon nanotube-based nanocomposite materials. Tartu, 2010, 147 p.
95. **Marko Kullapere.** Electrochemical properties of glassy carbon, nickel and gold electrodes modified with aryl groups. Tartu, 2010, 233 p.
96. **Liis Siinor.** Adsorption kinetics of ions at Bi single crystal planes from aqueous electrolyte solutions and room-temperature ionic liquids. Tartu, 2010, 101 p.
97. **Angela Vaasa.** Development of fluorescence-based kinetic and binding assays for characterization of protein kinases and their inhibitors. Tartu 2010, 101 p.
98. **Indrek Tulp.** Multivariate analysis of chemical and biological properties. Tartu 2010, 105 p.
99. **Aare Selberg.** Evaluation of environmental quality in Northern Estonia by the analysis of leachate. Tartu 2010, 117 p.
100. **Darja Lavõgina.** Development of protein kinase inhibitors based on adenosine analogue-oligoarginine conjugates. Tartu 2010, 248 p.
101. **Laura Herm.** Biochemistry of dopamine D_2 receptors and its association with motivated behaviour. Tartu 2010, 156 p.

102. **Terje Raudsepp.** Influence of dopant anions on the electrochemical properties of polypyrrole films. Tartu 2010, 112 p.
103. **Margus Marandi.** Electroformation of Polypyrrole Films: *In-situ* AFM and STM Study. Tartu 2011, 116 p.
104. **Kairi Kivirand.** Diamine oxidase-based biosensors: construction and working principles. Tartu, 2011, 140 p.
105. **Anneli Kruve.** Matrix effects in liquid-chromatography electrospray mass-spectrometry. Tartu, 2011, 156 p.
106. **Gary Urb.** Assessment of environmental impact of oil shale fly ash from PF and CFB combustion. Tartu, 2011, 108 p.
107. **Nikita Oskolkov.** A novel strategy for peptide-mediated cellular delivery and induction of endosomal escape. Tartu, 2011, 106 p.
108. **Dana Martin.** The QSPR/QSAR approach for the prediction of properties of fullerene derivatives. Tartu, 2011, 98 p.
109. **Säde Viirlaid.** Novel glutathione analogues and their antioxidant activity. Tartu, 2011, 106 p.
110. **Ülis Sõukand.** Simultaneous adsorption of Cd^{2+}, Ni^{2+}, and Pb^{2+} on peat. Tartu, 2011, 124 p.
111. **Lauri Lipping.** The acidity of strong and superstrong Brønsted acids, an outreach for the "limits of growth": a quantum chemical study. Tartu, 2011, 124 p.
112. **Heisi Kurig.** Electrical double-layer capacitors based on ionic liquids as electrolytes. Tartu, 2011, 146 p.
113. **Marje Kasari.** Bisubstrate luminescent probes, optical sensors and affinity adsorbents for measurement of active protein kinases in biological samples. Tartu, 2012, 126 p.
114. **Kalev Takkis.** Virtual screening of chemical databases for bioactive molecules. Tartu, 2012, 122 p.
115. **Ksenija Kisseljova**. Synthesis of aza-β^3-amino acid containing peptides and kinetic study of their phosphorylation by protein kinase A. Tartu, 2012, 104 p.
116. **Riin Rebane.** Advanced method development strategy for derivatization LC/ESI/MS. Tartu, 2012, 184 p.
117. **Vladislav Ivaništšev.** Double layer structure and adsorption kinetics of ions at metal electrodes in room temperature ionic liquids. Tartu, 2012, 128 p.
118. **Irja Helm.** High accuracy gravimetric Winkler method for determination of dissolved oxygen. Tartu, 2012, 139 p.
119. **Karin Kipper.** Fluoroalcohols as Components of LC-ESI-MS Eluents: Usage and Applications. Tartu, 2012, 164 p.
120. **Arno Ratas.** Energy storage and transfer in dosimetric luminescent materials. Tartu, 2012, 163 p.
121. **Reet Reinart-Okugbeni**. Assay systems for characterisation of subtype-selective binding and functional activity of ligands on dopamine receptors. Tartu, 2012, 159 p.

122. **Lauri Sikk.** Computational study of the Sonogashira cross-coupling reaction. Tartu, 2012, 81 p.
123. **Karita Raudkivi.** Neurochemical studies on inter-individual differences in affect-related behaviour of the laboratory rat. Tartu, 2012, 161 p.
124. **Indrek Saar.** Design of GalR2 subtype specific ligands: their role in depression-like behavior and feeding regulation. Tartu, 2013, 126 p.
125. **Ann Laheäär.** Electrochemical characterization of alkali metal salt based non-aqueous electrolytes for supercapacitors. Tartu, 2013, 127 p.
126. **Kerli Tõnurist.** Influence of electrospun separator materials properties on electrochemical performance of electrical double-layer capacitors. Tartu, 2013, 147 p.
127. **Kaija Põhako-Esko.** Novel organic and inorganic ionogels: preparation and characterization. Tartu, 2013, 124 p.
128. **Ivar Kruusenberg.** Electroreduction of oxygen on carbon nanomaterial-based catalysts. Tartu, 2013, 191 p.
129. **Sander Piiskop.** Kinetic effects of ultrasound in aqueous acetonitrile solutions. Tartu, 2013, 95 p.
130. **Ilona Faustova**. Regulatory role of L-type pyruvate kinase N-terminal domain. Tartu, 2013, 109 p.
131. **Kadi Tamm.** Synthesis and characterization of the micro-mesoporous anode materials and testing of the medium temperature solid oxide fuel cell single cells. Tartu, 2013, 138 p.
132. **Iva Bozhidarova Stoyanova-Slavova.** Validation of QSAR/QSPR for regulatory purposes. Tartu, 2013, 109 p.
133. **Vitali Grozovski**. Adsorption of organic molecules at single crystal electrodes studied by *in situ* STM method. Tartu, 2014, 146 p.
134. **Santa Veikšina**. Development of assay systems for characterisation of ligand binding properties to melanocortin 4 receptors. Tartu, 2014, 151 p.
135. **Jüri Liiv.** PVDF (polyvinylidene difluoride) as material for active element of twisting-ball displays. Tartu, 2014, 111 p.
136. **Kersti Vaarmets.** Electrochemical and physical characterization of pristine and activated molybdenum carbide-derived carbon electrodes for the oxygen electroreduction reaction. Tartu, 2014, 131 p.
137. **Lauri Tõntson**. Regulation of G-protein subtypes by receptors, guanine nucleotides and Mn^{2+}. Tartu, 2014, 105 p.
138. **Aiko Adamson.** Properties of amine-boranes and phosphorus analogues in the gas phase. Tartu, 2014, 78 p.
139. **Elo Kibena**. Electrochemical grafting of glassy carbon, gold, highly oriented pyrolytic graphite and chemical vapour deposition-grown graphene electrodes by diazonium reduction method. Tartu, 2014, 184 p.
140. **Teemu Näykki.** Novel Tools for Water Quality Monitoring – From Field to Laboratory. Tartu, 2014, 202 p.
141. **Karl Kaupmees.** Acidity and basicity in non-aqueous media: importance of solvent properties and purity. Tartu, 2014, 128 p.

142. **Oleg Lebedev**. Hydrazine polyanions: different strategies in the synthesis of heterocycles. Tartu, 2015, 118 p.
143. **Geven Piir.** Environmental risk assessment of chemicals using QSAR methods. Tartu, 2015, 123 p.
144. **Olga Mazina.** Development and application of the biosensor assay for measurements of cyclic adenosine monophosphate in studies of G protein-coupled receptor signalinga. Tartu, 2015, 116 p.
145. **Sandip Ashokrao Kadam.** Anion receptors: synthesis and accurate binding measurements. Tartu, 2015, 116 p.
146. **Indrek Tallo.** Synthesis and characterization of new micro-mesoporous carbide derived carbon materials for high energy and power density electrical double layer capacitors. Tartu, 2015, 148 p.
147. **Heiki Erikson.** Electrochemical reduction of oxygen on nanostructured palladium and gold catalysts. Tartu, 2015, 204 p.
148. **Erik Anderson.** *In situ* Scanning Tunnelling Microscopy studies of the interfacial structure between Bi(111) electrode and a room temperature ionic liquid. Tartu, 2015, 118 p.
149. **Girinath G. Pillai.** Computational Modelling of Diverse Chemical, Biochemical and Biomedical Properties. Tartu, 2015, 140 p.
150. **Piret Pikma.** Interfacial structure and adsorption of organic compounds at Cd(0001) and Sb(111) electrodes from ionic liquid and aqueous electrolytes: an *in situ* STM study. Tartu, 2015, 126 p.
151. **Ganesh babu Manoharan.** Combining chemical and genetic approaches for photoluminescence assays of protein kinases. Tartu, 2016, 126 p.
152. **Carolin Siimenson**. Electrochemical characterization of halide ion adsorption from liquid mixtures at Bi(111) and pyrolytic graphite electrode surface. Tartu, 2016, 110 p.
153. **Asko Laaniste.** Comparison and optimisation of novel mass spectrometry ionisation sources. Tartu, 2016, 156 p.
154. **Hanno Evard.** Estimating limit of detection for mass spectrometric analysis methods. Tartu, 2016, 224 p.
155. **Kadri Ligi.** Characterization and application of protein kinase-responsive organic probes with triplet-singlet energy transfer. Tartu, 2016, 122 p.
156. **Margarita Kagan.** Biosensing penicillins' residues in milk flows. Tartu, 2016, 130 p.
157. **Marie Kriisa.** Development of protein kinase-responsive photoluminescent probes and cellular regulators of protein phosphorylation. Tartu, 2016, 106 p.
158. **Mihkel Vestli.** Ultrasonic spray pyrolysis deposited electrolyte layers for intermediate temperature solid oxide fuel cells. Tartu, 2016, 156 p.
159. **Silver Sepp**. Influence of porosity of the carbide-derived carbon on the properties of the composite electrocatalysts and characteristics of polymer electrolyte fuel cells. Tartu, 2016, 137 p.
160. **Kristjan Haav**. Quantitative relative equilibrium constant measurements in supramolecular chemistry. Tartu, 2017, 158 p.

161. **Anu Teearu**. Development of MALDI-FT-ICR-MS methodology for the analysis of resinous materials. Tartu, 2017, 205 p.
162. **Taavi Ivan**. Bifunctional inhibitors and photoluminescent probes for studies on protein complexes. Tartu, 2017, 140 p.
163. **Maarja-Liisa Oldekop**. Characterization of amino acid derivatization reagents for LC-MS analysis. Tartu, 2017, 147 p.
164. **Kristel Jukk**. Electrochemical reduction of oxygen on platinum- and palladium-based nanocatalysts. Tartu, 2017, 250 p.
165. **Siim Kukk**. Kinetic aspects of interaction between dopamine transporter and *N*-substituted nortropane derivatives. Tartu, 2017, 107 p.
166. **Birgit Viira**. Design and modelling in early drug development in targeting HIV-1 reverse transcriptase and Malaria. Tartu, 2017, 172 p.
167. **Rait Kivi**. Allostery in cAMP dependent protein kinase catalytic subunit. Tartu, 2017, 115 p.
168. **Agnes Heering**. Experimental realization and applications of the unified acidity scale. Tartu, 2017, 123 p.
169. **Delia Juronen**. Biosensing system for the rapid multiplex detection of mastitis-causing pathogens in milk. Tartu, 2018, 85 p.
170. **Hedi Rahnel.** ARC-inhibitors: from reliable biochemical assays to regulators of physiology of cells. Tartu, 2018, 176 p.
171. **Anton Ruzanov.** Computational investigation of the electrical double layer at metal–aqueous solution and metal–ionic liquid interfaces. Tartu, 2018, 129 p.
172. **Katrin Kestav.** Crystal Structure-Guided Development of Bisubstrate-Analogue Inhibitors of Mitotic Protein Kinase Haspin. Tartu, 2018, 166 p.
173. **Mihkel Ilisson.** Synthesis of novel heterocyclic hydrazine derivatives and their conjugates. Tartu, 2018, 101 p.
174. **Anni Allikalt.** Development of assay systems for studying ligand binding to dopamine receptors. Tartu, 2018, 160 p.
175. **Ove Oll.** Electrical double layer structure and energy storage characteristics of ionic liquid based capacitors. Tartu, 2018, 187 p.
176. **Rasmus Palm.** Carbon materials for energy storage applications. Tartu, 2018, 114 p.
177. **Jörgen Metsik.** Preparation and stability of poly(3,4-ethylenedioxythiophene) thin films for transparent electrode applications. Tartu, 2018, 111 p.
178. **Sofja Tšepelevitš.** Experimental studies and modeling of solute-solvent interactions. Tartu, 2018, 109 p.
179. **Märt Lõkov.** Basicity of some nitrogen, phosphorus and carbon bases in acetonitrile. Tartu, 2018, 104 p.
180. **Anton Mastitski**. Preparation of α-aza-amino acid precursors and related compounds by novel methods of reductive one-pot alkylation and direct alkylation. Tartu, 2018, 155 p.
181. **Jürgen Vahter**. Development of bisubstrate inhibitors for protein kinase CK2. Tartu, 2019, 186 p.

182. **Piia Liigand.** Expanding and improving methodology and applications of ionization efficiency measurements. Tartu, 2019, 189 p.
183. **Sigrid Selberg.** Synthesis and properties of lipophilic phosphazene-based indicator molecules. Tartu, 2019, 74 p.
184. **Jaanus Liigand.** Standard substance free quantification for LC/ESI/MS analysis based on the predicted ionization efficiencies. Tartu, 2019, 254 p.
185. **Marek Mooste.** Surface and electrochemical characterisation of aryl film and nanocomposite material modified carbon and metal-based electrodes. Tartu, 2019, 304 p.
186. **Mare Oja.** Experimental investigation and modelling of pH profiles for effective membrane permeability of drug substances. Tartu, 2019, 306 p.
187. **Sajid Hussain.** Electrochemical reduction of oxygen on supported Pt catalysts. Tartu, 2019, 220 p.
188. **Ronald Väli.** Glucose-derived hard carbon electrode materials for sodium-ion batteries. Tartu, 2019, 180 p.
189. **Ester Tee.** Analysis and development of selective synthesis methods of hierarchical micro- and mesoporous carbons. Tartu, 2019, 210 p.
190. **Martin Maide.** Influence of the microstructure and chemical composition of the fuel electrode on the electrochemical performance of reversible solid oxide fuel cell. Tartu, 2020, 144 p.
191. **Edith Viirlaid.** Biosensing Pesticides in Water Samples. Tartu, 2020, 102 p.
192. **Maike Käärik.** Nanoporous carbon: the controlled nanostructure, and structure-property relationships. Tartu, 2020, 162 p.
193. **Artur Gornischeff.** Study of ionization efficiencies for derivatized compounds in LC/ESI/MS and their application for targeted analysis. Tartu, 2020, 124 p.
194. **Reet Link.** Ligand binding, allosteric modulation and constitutive activity of melanocortin-4 receptors. Tartu, 2020, 108 p.
195. **Pilleriin Peets.** Development of instrumental methods for the analysis of textile fibres and dyes. Tartu, 2020, 150 p.
196. **Larisa Ivanova.** Design of active compounds against neurodegenerative diseases. Tartu, 2020, 152 p.
197. **Meelis Härmas.** Impact of activated carbon microstructure and porosity on electrochemical performance of electrical double-layer capacitors. Tartu, 2020, 122 p.
198. **Ruta Hecht.** Novel Eluent Additives for LC-MS Based Bioanalytical Methods. Tartu, 2020, 202 p.
199. **Max Hecht.** Advances in the Development of a Point-of-Care Mass Spectrometer Test. Tartu, 2020, 168 p.
200. **Ida Rahu.** Bromine formation in inorganic bromide/nitrate mixtures and its application for oxidative aromatic bromination. Tartu, 2020, 116 p.
201. **Sander Ratso**. Electrocatalysis of oxygen reduction on non-precious metal catalysts. Tartu, 2020, 371 p.
202. **Astrid Darnell.** Computational design of anion receptors and evaluation of host-guest binding. Tartu, 2021, 150 p.

203. **Ove Korjus.** The development of ceramic fuel electrode for solid oxide cells. Tartu, 2021, 150 p.
204. **Merit Oss.** Ionization efficiency in electrospray ionization source and its relations to compounds' physico-chemical properties. Tartu, 2021, 124 p.
205. **Madis Lüsi**. Electroreduction of oxygen on nanostructured palladium catalysts. Tartu, 2021, 180 p.
206. **Eliise Tammekivi.** Derivatization and quantitative gas-chromatographic analysis of oils. Tartu, 2021, 122 p.
207. **Simona Selberg.** Development of Small-Molecule Regulators of Epi-transcriptomic Processes. Tartu, 2021, 122 p.